ROBUST

LOCATION DETERMINATION

IN WIRELESS AD-HOC NETWORKS

A Thesis

Submitted to the Faculty

of

Purdue University

by

Nipoon Malhotra

In Partial Fulfillment of the

Requirements for the Degree

of

Master of Science in Electrical and Computer Engineering

August 2004

To my family for their support and guidance

ACKNOWLEDGEMENTS

Special thanks to Dr. Bagchi for his apt guidance and insightful inputs which led to the completion of this thesis. His unflinching optimism and hard work were a constant source of inspiration that motivated me to work for the fruition of this research effort. I must also thank Serdar Cabuk, Mark Krasniewski and Bingrui Foo for their contribution to this research work.

TABLE OF CONTENTS

Page

LIST OF TABLES

LIST OF FIGURES

ABSTRACT

Malhotra, Nipoon. M.S. in ECE, Purdue University, August 2004. Robust Location Determination in Wireless Ad-Hoc Networks. Major Professor: Saurabh Bagchi.

With the development of location aware applications for ad-hoc and sensor networks, location determination has become an important middleware technology. Cost, size, and energy constraints permit only a fraction of the network nodes, called anchors, to carry location determination hardware such as GPS receivers.

The first part of our work involves evaluating the effect of topological characteristics, such as coverage and connectivity, on the accuracy of location determination protocols. We study a protocol called Hop-Terrain that uses the received signal strength from anchors for estimating position of sensor nodes. The resultant performance predictions can be used in motion planning for nodes to improve the accuracy of location estimates.

An emerging trend in sensor networks is deploying directional RF antennas on nodes due to advantages like energy conservation and better bandwidth utilization. The location estimation techniques for omni-directional antennas cannot be employed in such systems since the received power at a node depends on additional variables like transmission and receiving angles. Our work presents techniques for location determination with directional antennas under different kinds of node deployments, such as globally aligned nodes and unaligned nodes. We show how the problem can be solved in a two-dimensional plane by using just one anchor in contrast to three anchors for omni-directional antennas. We consider the possibility of errors in individual distance measurements and present theoretical as well as simulation-based results for the level of

redundancy required to have an aggregate estimation error below a desired threshold. Simulations show improvement in the accuracy of the position estimates over that of the triangulation based approach for omni-directional antennas.

1. INTRODUCTION

Mobile Ad-hoc Networks (MANETs) consist of mobile hosts that are connected by wireless links to form a self-configuring network. These hosts also act as routers, thus enabling multi-hop communication.

Sensor networks are a particular class of ad-hoc networks designed for collecting information about the physical environment in which they are deployed. These networks consist of tiny nodes equipped with micro-electro-mechanical (MEMS) components that include sensors, actuators and Radio Frequency (RF) transceivers. Nodes may also have signal processing engines for supporting communication protocols or processing sensed data. Typical sensor nodes have limited processing capabilities but are capable of supporting relatively complex distributed applications through coordinated effort. Sensor nodes are usually battery-powered. Since frequent battery replacements are difficult, reducing energy consumption is an important design consideration for sensor networks. Energy considerations also limit the transmission range of sensor nodes as the transmission range in free space is proportional to the square root of the transmitted power. As a result, most sensor nodes are only capable of short range communication up to a few hundred feet.

Large scale sensor networks can consist of hundreds or even thousands of nodes dispersed over a sensor field. Individual nodes gather data from their respective sensing fields. The collected data is transmitted to a data aggregation point such as a base station or a cluster head for further analysis. In a large number of applications, interpretation of the sensed data requires knowledge of the location of the sensing node. This includes common applications such as studying weather conditions in a habitat, tracking migration patterns of an endangered species, early warning system for floods, military surveillance etc. Such applications require that sensors transmit their location coordinates along with the sensed data. But location information is not readily available at these sensing nodes because sensor nodes are often randomly dispersed over a sensor field. Location information is also not available at a node for the important class of mobile sensor networks in which the nodes move in a controlled manner or through passive mobility. Controlled mobility implies that a node moves of its own volition through being mounted on some actuators, such as robots, and the movement can be controlled. Passive mobility implies the node moves without control. This kind of movement may happen if the node is embedded in some animals that move about as in [1], or if the node is light and can be carried by some physical phenomenon, such as air or moving water.

It is possible for a node to have up-to-date information of its location if it has some location determination hardware, such as a GPS receiver, mounted on it. It is usually not feasible to equip each sensor node with such specialized hardware for a variety of reasons. A key design principle for many sensor network applications is that they should be scalable to large network sizes. From an economic standpoint, the deployments should be cost-effective. Such economic considerations have been driving the cost of the individual sensor nodes down to the point where sub-$1 nodes are beginning to look achievable [2], but the GPS hardware increases the price of sensor networks substantially. Commercially available GPS receivers come in a wide price range of $10-$10,000. The receivers at the lowest end give poor accuracy, with errors of the order of tens of meters [3]. The receivers that give sub-meter accuracy, which may be needed for many sensor applications, currently cost more than $5,000. The hardware also adds to the weight of the unit with typical receivers weighing upwards of 5 oz. Moreover, the battery life of GPS receivers is much shorter than that of the sensor nodes, e.g., of the order of tens of hours for typical GPS receivers compared to a few months for a representative sensor node such as the Berkeley mote. Thus, the combined unit consisting of the sensor node and the GPS receiver will require far too frequent battery replacements for it to be practical. More generally, the received signal strength for a GPS can be as low as -130 dBm. This is orders of magnitudes less than the strength of signals used for communication in terrestrial applications and is lower than the sensitivity of receivers on typical sensor nodes (-98 dBm on the representative Berkeley sensor motes). Therefore expensive receivers would be needed for such an arrangement for location determination. Finally, because relatively unobstructed views are required for GPS localization, in many sensor network deployments, the GPS measurements would need to be supplemented with ranging data from the local network. This includes deployments in forests with foliage cover above the ground and deployments in indoors environments.

Though it may not be feasible for all the nodes to be equipped with special purpose location determination hardware, it is possible to equip a small fraction of the nodes in a network with such hardware. These special nodes, henceforth called *anchor nodes*, can act as reference points for deriving location information. Other nodes, called *target nodes* or simply *sensor nodes*, can determine their location by estimating relative distances from multiple anchor nodes. In the most commonly used technique called *lateration* distance measurements from ($k+1$) anchors in a k-dimensional plane are required for location determination. The instance of lateration in a 2-dimensional plane is called *triangulation* in which a sensor node needs to know its distances from three neighboring anchors. Several approaches exist for estimating this distance from neighbors e.g. signal strength attenuation and time of flight. In the signal strength attenuation based technique, the power of received signal is measured by the sensor node. With a knowledge of the signal strength emitted by the source node and the attenuation relationship with distance (such as $1/r^2$ where r is the distance traveled by signal), the inter-node distance can be calculated. For indoor environments or large distances, the attenuation relationship becomes complex and difficult to represent concisely because of multi-path effects and reflection of the radio waves. Other techniques for measuring inter-node distances, such as time of flight ([4][5]), are less useful in our environment because the radio signals travel at the speed of light and the distances traveled by these signals are relatively short.

A useful metric for comparing the efficacy of the wide variety of existent location determination techniques is the average error in location estimates of sensor nodes. Apart from the choice of the protocol used, the accuracy of location estimation depends on the topology of the sensor network under consideration. Topological characteristics such as connectivity, coverage and diameter of a network affect the performance of application layer protocols including those for location determination. Knowledge of the effect of topology on these protocols can be useful for deployment of sensors in an efficient fashion. In networks where controlled mobility is possible this can be used for motion planning to move nodes in an optimal topological configuration. In [6] Bagchi *et. al.* propose a technique based on intelligent motion of sensor nodes that can be used to position nodes in a manner that achieves desired values of topological characteristics including connectivity, coverage and diameter. This technique uses different kinds of motion algorithms each having a specific effect on the network topology e.g. decreasing network diameter or increasing network coverage. Based on a network's requirements an appropriate motion algorithm is applied to change the network's topological characteristics to desired values in small incremental steps. It is claimed that enhancing one or multiple of these topological characteristics to suit the requirements of an application layer protocol can lead to improved Quality of Service (QoS). In the first part of this thesis, we apply the above intelligent motion algorithm to sensor networks and evaluate the improvement in accuracy of location determination. We employ a popular location determination protocol called Hop-Terrain and Refinement [7] for this study. Our simulation based studies show that an appropriate choice for the set of topological characteristics can improve accuracy of location determination by up to 68%.

The Hop-Terrain algorithm studied in the first part of this thesis is designed for sensor nodes equipped with omni-directional antennas. It uses measurement of received power at a sensor node in conjunction with the knowledge of power transmitted by an anchor for estimating inter-node distance. A model that assumes that the received power falls off as the square of the distance between the transmitter and the receiver is used. This is a common technique used in a variety of location determination schemes ([8][9][10][11][12]). In spite of being simple and elegant this model is not always applicable because of the increasing number of sensor systems that deploy directional antennas. Use of these directional antennas provides important benefits in sensor networks. Directionality can be used as a form of diversity built into sensor nodes, which helps in coping with undesirable variability in the communication channel such as noise. Diversity is a means of introducing redundancy in a system by equipping it with multiple means of performing a single operation. Using multiple directional antennas in a diversity configuration makes communication more robust because even if channel noise corrupts the transmitted signal along one path, the signal received at other antennas along a different set of paths can be used for decoding the transmitted message. Directionality also provides increased transmission range compared to omni-directional antennas by focusing the transmission energy in the direction of the receiver. Directional antennas can also enhance the security of communication by restricting the set of neighbors that can overhear a communication [13]. Directionality in expensive communication systems is commonly achieved through the creation of a phased array. However, this is prohibitively expensive for sensor networks and is used predominantly for high cost military applications. In addition, it is required by the laws of physics that the elements of the phased array be an appreciable fraction of a wavelength apart. This is not possible in electrically small form factor sensor nodes. This precludes the use of a traditional array to provide the desired beam scanning. However limited directionality can be cheaply integrated into a small form factor sensor node. Reduced size patch antennas have been developed using novel patch arrangements and high dielectric constant antennas. Multiple patch antennas oriented along different directions can be deployed on sensor nodes. A simple switching network enables the switch between polarization states ([1][14]) and the direction of radiation.

The solutions to the location determination problem using omni-directional antennas are inapplicable to systems employing directional antennas. This is because the received power at a sensor is a function of the transmitted power, the inter-node distance as well as the transmitting and receiving angles. There are three unknowns involved and the distance between the anchor and the sensor cannot be estimated from this single relation. In this thesis we propose a set of techniques that solve this problem. As our model for sensor nodes we use nodes that are equipped with four directional antennas. Each of these antennas points towards one quadrant of a 360˚ (2B) field. Depending on the deployment scenario, the beam-width of each of these antennas varies from 90˚ (B/2) to 180˚ (B). We show that a sensor node can estimate its location using information from a single anchor in the ideal case. The triangulation method for omni-directional antennas, in contrast, uses three anchor nodes in the ideal case for a two dimensional plane. The ideal case is when there is no error in the estimation of relative distances. For erroneous range measurements information from a redundant number of anchors is combined by a method called *Error Resilient Triangulation (ERT)* ([7][15]). It is an extension of triangulation that employs a redundant set of linear equations that are solved to minimize the least square error. In our approach, the multiple location estimates from different anchors are averaged to determine the target node's location. We build a simulation model with random locations of anchor nodes and two possible placements of the nodes – an aligned placement where all the nodes are aligned along some arbitrary coordinate axes and an unaligned placement that may result from some rapid deployment of the nodes, such as through air dropping. We show through simulation that the aggregate error is reduced through the use of our technique compared to the ERT method. The improvement in accuracy ranges between 2 to 7 times depending on the number of neighbors and the error in input measurements.

It should be noted that standard, small form-factor, sensor nodes rarely have a truly omni-directional antenna pattern even if a simple dipole is implemented because of ground plane asymmetry. While the radiating portion of the antenna is often circularly symmetric, the rest of the mote radiates from parasitic currents resulting in asymmetric patterns ([16]). As a result, the signal does not strictly attenuate as $1/r^2$ where r is the propagation distance. This is a major source of error in the previously mentioned power measurement based localization schemes that assume omni-directional antennas. Directional antennas are more resistant to such errors.

2. RELATED WORK

As outlined in the previous section, location determination is a fairly important problem in sensor networks and a variety of solutions have been proposed for this. While topological characteristics of networks have been extensively studied, the effect of topological characteristics on the performance of applications such as location determination has not been thoroughly explored. In this section, we describe some of the prior research in these areas.

2.1 Topological Characteristics of Sensor Networks

Studies have been conducted in the past to find the relationship between network design parameters and characteristics of the resulting networks.

2.1.1 Effect of design parameters on topological characteristics

A previous work by Jensen *et. al.* [16] investigates the transmission range necessary for having a fully connected sensor network. This provides probabilistic upper and lower bounds on the network connectivity achievable for a given value of the transmission radius. A relation between sensor density and connectivity is also provided. The authors claim that providing probabilistic bounds on connectivity instead of deterministic bounds leads to significant energy savings. However, the possible adverse affects of such probabilistic bounds on performance of higher layer protocols have not been investigated. Another work [17] provides the range and sensor density requirements for achieving desired connectivity and node degree. These studies were done for static networks and have not considered the effects of node mobility on system performance. In addition these studies do not incorporate the possibility of transient or permanent node failures in their model. This limits their applicability as failures will cause requirements for desirable topological characteristics to be harsher compared to the theoretical predictions. In a study by Bettstetter [18] connectivity, diameter and coverage of a network have been analyzed. The effect of node failures has been studied but only static nodes have been considered. These studies either fail to account for the performance enhancement that can be achieved by controlled goal directed motion of sensor nodes or do not model node failures.

2.1.2 Effect of controlled mobility on topological characteristics

In applications where sensors are mounted on mobile agents with controlled mobility, the motion of nodes can be used to achieve desirable topological traits. Howard *et. al*. [20] present a distributed algorithm for maximizing the coverage area of a sensor network. The algorithm works by assigning a virtual repulsive field to all sensor nodes as well as obstacles in the system. The nodes move to minimize the virtual potential created by this field. This behaves like the electrostatic field of a point charge and spreads the nodes away from each other and in the process increases coverage. A friction force is also introduced to ensure convergence to a stable equilibrium. Though this algorithm ensures an increase in coverage, it can lead to loss of connectivity in the network.

In a work by Butler *et. al.* [21], a technique is proposed to optimize the deployment of sensors based on the spatial distribution of the occurrence of events of interest. In this scheme nodes tend to concentrate around locations where events of interest occur frequently. This selective increase in sensor density makes the system more robust to node failures as regions of high activity have more redundant nodes to take up the sensing responsibilities of faulty nodes. The algorithm also uses heuristics that prevent loss of network connectivity.

A new type of sensor network consisting of a combination of mobile and static nodes is proposed in [22]. The static nodes are randomly deployed and this can lead to coverage holes in the network. The mobile nodes move to these holes to enhance the overall network coverage.

These techniques are mainly designed to optimize one network characteristic and do not consider the tradeoff between different traits such as coverage and diameter e.g. a sensor network's coverage can be increased by spreading the nodes but this can lead to a large network diameter or loss of connectivity. These techniques also do not provide a direct control over the values of topological characteristics.

Bagchi *et. al.* [6] present an algorithm for node mobility that can be used to simultaneously achieve desired values for a set of network characteristics. The system model accounts for both transient and permanent node failures. Theoretical as well as simulation based results are provided that predict the sensor densities required for simultaneously achieving a given combination of connectivity, coverage and diameter values. We use this algorithm as our tool for studying the effect of a network's topological characteristics on the performance of location determination techniques. For our study the intelligent motion algorithm is applied to practical node deployments and the accuracy of location determination in the resultant networks is measured. This is described in more detail in section 3.

2.2 Techniques for Location Determination

Triangulation is one of the most commonly used techniques for location determination in sensor networks. It uses the geometrical properties of a Euclidean space to solve for the location of an object using measurements of its distance from other objects of known location. This is applicable to sensor networks where some sensor nodes are equipped with GPS receivers and know their locations. An overview of triangulation based location determination techniques can be found in [23] and [24]. The triangulation techniques can be sub-divided into two categories – *lateration*, which uses distance measurements, and *angulation*, which uses angle measurements in addition to distance measurements.

Lateration to uniquely solve for a point in an *n*-dimensional space requires a consistent system of (*n+1*) independent equations. This translates to the fact that lateration in an *n*-dimensional plane requires (*n+1*) neighbors with knowledge of their location. This assumes that the individual distance measurements are completely accurate and an absence of singular cases such as three or more points on a line. An example of lateration in two-dimensional space is shown in Fig. 2.1(a). Domain specific knowledge may be used to reduce the number of distance measurements needed. For example, the Active Bat Location System [25] locates mobile tags, called Bats, using a grid of ultrasound sensors mounted on the ceiling using only 3 sensors in 3 dimensions because it is known that the bats are all placed below the sensors.

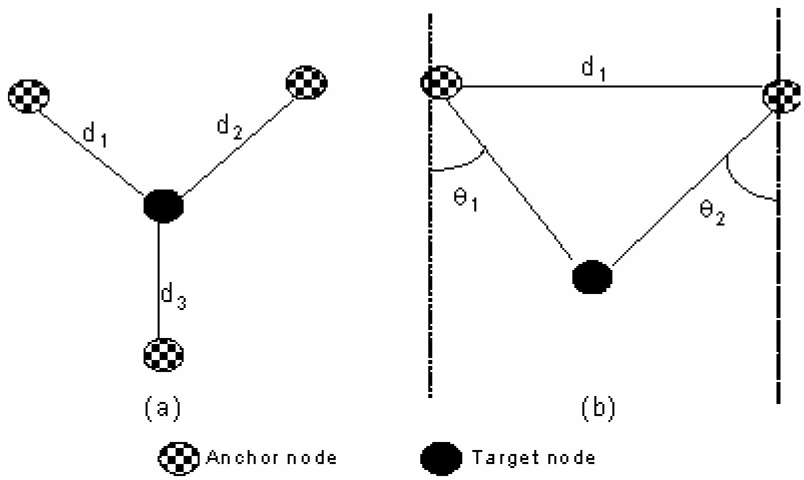

Fig. 2.1 Location determination using lateration in (a) and angulation in (b)

Several methods have been proposed for obtaining estimates of the distance from neighbors that are required for triangulation in sensor networks. These include techniques based on measuring the time of flight, attenuation of signal strength, and directionality ([24][26]). The time of flight technique is based on measuring the time it takes to traverse an unknown distance with a known velocity. If neighbors are approximately stationery, inter-node distance can be estimated by observing the difference in transmission and arrival time of an emitted signal. This is not suitable for typical sensor networks as RF signals travel at the speed of light and the distances for wireless communication are usually a few tens of meters. Measuring signal strength relies on the property that radio waves attenuate with increasing distance between the transmitter and the receiver. The receiver can calculate its distance from the transmitter if it knows the transmission power and the attenuation model. Radio signal attenuation can be fairly accurately modeled as a *1/r*^{2} decrease in power i.e. $P_{received} = P_{transmitted}/r^2$, where *r* is a relatively short distance in outdoors environment. This gives inaccurate indoor distance estimates because the model does not adequately represent the effects of reflections and multi-path fading. The received signal strength technique is used in the SpotON ad-hoc location system that implements attenuation measurement using low-cost tags [27]. The third way of estimating location is to compute the angle of each reference point with respect to the sensing node in some reference frame. The position of the mobile node can then be computed using angulation.

In practice, the individual distance measurements are inaccurate because the exact relation between the measurement of physical properties, such as signal strength, and the inter-node distance is not known. Errors in range estimates could also result due to malicious nodes. These nodes can exhibit *Byzantine failures* and result in arbitrary range estimates. Hence, information from greater than (*n+1*) nodes is needed for pinpointing a target node in an *n*-dimensional plane. The work in [15] presents an approach for minimizing the aggregate error by considering measurements from a redundant number of anchor nodes. Consider that the target node's distance from *k* neighbors is known. These neighbors need not be one-hop neighbors. In a 3-dimensional space, let the position of neighbor *i* be (x_i, y_i, z_i). Let the location of the target node that needs to be determined be (u_x, u_y, u_z). If distance of the target node from neighbor *i* is d_i then, $(x_i - u_x)^2 + (y_i - u_y)^2 + (z_i - u_z)^2 = d_i^{\,2}$. This structure can be linearized [7] to give the relation $Au = b$ where

$$A = -2\begin{bmatrix} x_1 - x_k & y_1 - y_k & z_1 - z_k \\ x_2 - x_k & y_2 - y_k & z_2 - z_k \\ \cdots & \cdots & \cdots \\ x_{k-1} - x_k & y_{k-1} - y_k & z_{k-1} - z_k \end{bmatrix}, u = \begin{bmatrix} u_x \\ u_y \\ u_z \end{bmatrix}$$

$$b = \begin{bmatrix} d_1^{\,2} - d_k^{\,2} - x_1^{\,2} + x_k^{\,2} - y_1^{\,2} + y_k^{\,2} - z_1^{\,2} + z_k^{\,2} \\ d_2^{\,2} - d_k^{\,2} - x_2^{\,2} + x_k^{\,2} - y_2^{\,2} + y_k^{\,2} - z_2^{\,2} + z_k^{\,2} \\ \cdots \\ d_{k-1}^{\,2} - d_k^{\,2} - x_{k-1}^{\,2} + x_k^{\,2} - y_{k-1}^{\,2} + y_k^{\,2} - z_{k-1}^{\,2} + z_k^{\,2} \end{bmatrix}$$

Solving this system of equations to minimize the least squares error gives

$$u = (A^T A)^{-1}.A^T b$$

This method forms the basis of the error resilient triangulation technique that Savarese *et al.* use for the protocol proposed in [7]. They propose an iterative protocol that diffuses the location information gathered from anchor nodes through the network. The protocol runs in two phases – the *Hop-Terrain* phase where initial estimates are gathered from the anchor nodes and the *Refinement* phase where the estimates are refined by making the nodes that have acquired rough location estimates using Hop-Terrain to act as anchor nodes.

Angulation is an alternate method to lateration for computing location based on neighbor information. To perform angulation in a two dimensional plane, two angle measurements and one length measurement, such as the distance between two anchor nodes, are needed. A schematic of angulation is shown in Fig. 2.1(b). In three dimensions, one length measurement, one azimuth measurement and two angle measurements are needed. Directional antennas are needed for the angle measurements. Previous work has employed phased antenna arrays for implementing the angulation technique [23]. Multiple antennas with known separation measure the time of arrival of a signal. Given the differences in arrival times and the geometry of the receiving array, it is then possible to compute the angle from which the emission originated. If there are enough elements in the array and large enough separations, the angulation calculation can be performed.

There is a class of location determination techniques that do not rely on any property of the received signal. Instead, they rely on the connectivity measure, i.e., if a node α is able to hear from another node β, then α is *connected* to β and its location is constrained to be within the transmission range of β ([26][28][29]). In [26], a set of reference points is chosen and each reference node sends out a beacon periodically. Each target node maintains a connected set that consists of all the reference nodes to which it is connected. If greater than a fraction of beacons sent out by a reference node are received at a particular target node, the target node adds the reference node to its connected set. Finally, after collecting information from all the reference nodes, the target node estimates its position as the centroid of the positions of the reference nodes in its connected set. In [28], Ramanathan *et. al.* use an iterative method to refine the possible locations of a target node based on the set of locations where a neighbor of the node can be, and the set of locations where a non-neighbor can be. The sets are computed based on *hello* messages periodically sent out by each node. In [29], Doherty *et. al.* model the peer-to-peer connection in a wireless sensor network as a set of geometric constraints on the node positions. The constraints become convex with directional transmitters and receivers that can sweep through an angle. The global solution of a feasibility problem for these constraints yields estimates for the positions of all nodes in the network. The estimates provide a rectangular bound around the possible position of a node. It is shown that as the constraints become tighter, the area of the bounding rectangle decreases. Also, using a variable transmission radius instead of a fixed radius improves performance.

This class of techniques based on connectivity measures provides location estimates that are coarse-grained. The granularity becomes coarser if the transmission range of the reference nodes is increased. An overhead of beacon or hello messages is also incurred and the convergence times of the algorithms are often sensitive to the frequency of these messages [29]. Also, some of the protocols ([28][29]) require centralized processing that limits their scalability.

Römer [30] proposes a technique geared to dust-sized sensor nodes that only have passive optical communication capability and do not have active RF communication capability. It relies on a powerful base station, called a *lighthouse* in the paper, which sends a photo beam and rotates. Each sensor node has a photo beam detector and a clock. The sensor nodes record how long they see the photo beam and the period of rotation and determine their location based on this. The method is only applicable if single hop communication is possible between all nodes and the base station.

Among the techniques described above, triangulation provides the highest granularity in position estimation without the need for complex centralized calculations. The use of received signal strength is the most widely applicable technique for estimating the inter-node distances required for triangulation. Even though the distance estimates thus obtained are inaccurate, the overall accuracy of the technique can be significantly improved by using error resilient triangulation. Because of the efficacy of the protocol proposed in [7] which is based on this scheme, we use it as a representative protocol for studying location determination.

3. EFFECT OF NETWORK TOPOLOGY ON LOCATION DETERMINATION

In this section we describe the implementation of a simulation model for evaluating the effect of a sensor network's topological characteristics on accuracy of location determination. The protocol that is considered for this study is the Hop-Terrain and Refinement protocol of Savarese *et. al.*[7]. Our simulations show that significant performance improvements are possible by modifying the topological placement of sensor nodes without having to increase the node density. But first, we describe the two protocols used for this study i.e. Hop-Terrain and Refinement protocol [7] and the *intelligent motion algorithm* [6].

3.1 Intelligent Motion Algorithm

Bagchi *et. al.* [6] propose an intelligent motion technique for sensor networks consisting of nodes capable of controlled mobility. Their motion algorithm moves the sensor nodes in such a fashion that the network topology is modified to simultaneously satisfy pre-defined constraints on connectivity, coverage and diameter. The basic technique used by the authors is to use a set of local motion patterns that when applied to each of the nodes help achieve certain global objectives such as reducing network diameter or increasing network coverage. Next, an evaluation function is defined that measures the deviation of the current network characteristics from the desired topological characteristics. Based on this evaluation function a topological characteristic that requires improvement is determined. The corresponding motion pattern is applied to the network nodes followed by recalculation of the evaluation function. This process is repeated until the desired topological constraints are met. If the desired characteristics are not achieved even after a large number of iterations, a failure is reported. Although this technique assumes that controlled node mobility is possible, it is equally applicable to a study of static networks. The intelligent motion algorithm can be applied to a random placement of nodes with the set of desired topological traits as inputs. The topology resulting from the application of this algorithm provides an optimal way of placing the sensor nodes at the time of deployment. The details of the different components of this scheme are as follow

3.1.1 Network parameters

One of the foremost requirements for any study of the topological characteristics of a network is to define the parameters of interest in a meaningful and consistent manner. In addition, it is preferable if this definition leads to parameters that are easy to measure.

The definition of connectivity used by the authors is based on the size of the largest connected component. The network is considered as an undirected graph with the sensors as its nodes. Sensors that are one hop neighbors are connected by edges in the graph. If the connected components in an n node graph are $C_1, C_2, C_3 \ldots C_k$ in the decreasing order of their sizes $G_1, G_2, G_3 \ldots G_k$ then the *connectivity* is defined as G_1/n. The length of the longest path having no cycles in this graph is defined as the network *diameter*.

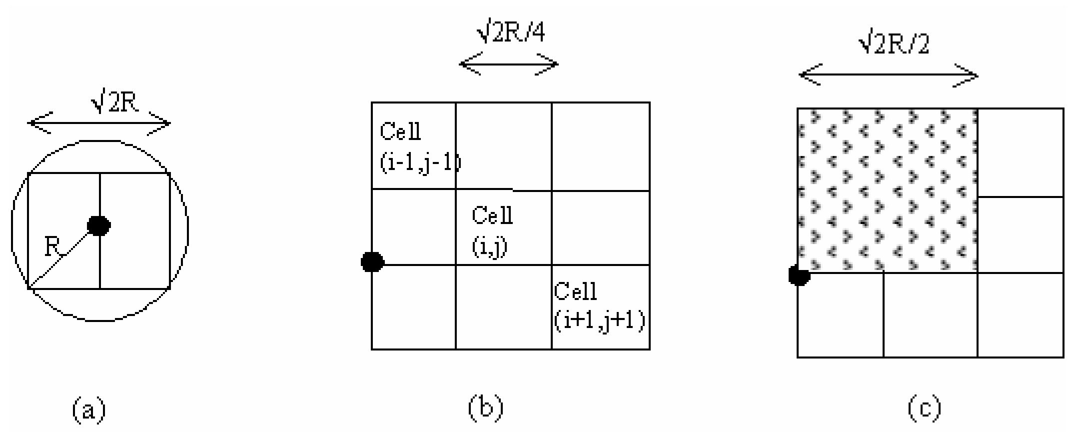

Fig. 3.1 Coverage Estimation

Traditionally network *coverage* has been defined as the percentage of the sensor field that is covered by the sensing area of at least one sensor node. The authors use a modified definition of coverage to provide a lower bound on this parameter. The sensing area of a node is approximated by a squares of side $\sqrt{2}*R$ (*square sense region*) where R is the sensing radius of the network nodes. This square is circumscribed by a circle of radius R which is the actual sensing area of a sensor node as shown in Fig. 3.1(a). To estimate coverage of the sensor field, it is divided into square cells of side $\sqrt{2}*R/4$ each as shown in Fig. 3.1(b). Any such cell is covered if there is a node in either that cell or in any of the 8 neighboring cells. To understand this, consider a node placed at the grid point shown in Fig. 3.1(c). It completely covers a square region of side $\sqrt{2}*R/2$ that is one quadrant of its square transmission region from Fig. 3.1(a). Therefore the entire cell (i, j) is covered by this node. The coverage of the network is given by the fraction of cells covered by the total number of cells in the sensing field. This definition of coverage gives a lower bound on the actual network coverage while greatly simplifying the coverage calculation for simulations.

3.1.2 System model

All nodes are considered to have a uniform and constant transmission range. The sensing radii of all the nodes are also same but the sensing radius can be different from the transmission range. The possibility of failures of nodes has also been modeled. Nodes can either have transient or permanent failures. The inter-arrival time of the node failures follows an exponential distribution with a mean which is a control parameter. The recovery time of the nodes for transient failures is also generated from an exponential distribution. The parameters of the system model can be changed to match the design parameters of the network under study.

3.1.3 Goal-driven mobility algorithms

The proposed algorithm for motion has the objective of meeting the requirements of coverage, connectivity, and diameter simultaneously. The connectivity and coverage requirements bound the allowable values from below (e.g., connectivity must be greater than 90%), while the diameter requirement bounds it from above. The algorithm runs iteratively and at each step, it chooses one of two possible mobility models depending on which metric has been satisfied and which needs to be improved.

The first mobility model is meant to decrease diameter and is called the *Mean Shift Clustering* (MSC) algorithm. Consider a naive motion pattern, called *Baseline MSC*, of moving a node to the centroid of all its neighbors that are up to *k* hops away. The sum of the distances of a node from its *k* and less hop neighbors is minimized by the motion. This has the potential of decreasing the diameter of the network if the longest path was through the node being moved to one of its k or less hop neighbors. However, the result of the motion would be that all the nodes would collapse to a single point and lead to negligible coverage. The model used by the authors for decreasing diameter is suggested by this naive model, but preserves coverage. Instead of moving a node to the centroid, it is moved a fraction of the distance and then the move is evaluated using an evaluation function. The evaluation function, henceforth called a *local evaluation function (LEF)* is given by:

*LEF = w1 * sum of distances from its k and less hop neighbors*
*– w2 * distance from centroid*

If the LEF gives a negative value, the node is not moved. Intuitively, for high coverage, the nodes should be spread out and the first term should be higher. When the nodes come too close to each other the first term becomes small causing LEF to be negative. This causes the node to remain static thus preventing a drastic reduction in coverage. Depending on which of the parameters amongst diameter and coverage has already been satisfied, the values of *w1* and *w2* can be adjusted. For normalization, instead of absolute values, relative changes are considered from the previous value.

The second mobility model is meant to increase connectivity and coverage. It is called the *Shift Neighbors Away* (SNA) algorithm. This algorithm can be thought of as sweeping through the sensor field, once from left to right starting at the top and next from right to left starting at the bottom pushing the nodes away from each other without disconnecting two immediate neighbors. In the sweep from left to right, when a node *i* is considered, all the nodes in the fourth quadrant of its square sense region (SSR) are pushed away from the center of node *i*. A neighbor can be pushed a maximum of *r* (transmission range) distance away without disconnection. However, to avoid the situation of many nodes squished at the bottom of the field, the push is a fraction *f* of *r*. The fraction *f* is a decreasing function of the number of nodes. The working of the algorithm is shown schematically for two nodes *i* and *j* in Fig. 3.2. Node *i* is the node under consideration in the algorithm and node *j* is the neighbor that is to be pushed away. A similar process is followed when the sweep is done from the right to the left starting at the bottom. The intelligent motion algorithm executes either MSC followed by SNA, or only SNA depending on whether diameter constraints have been satisfied or not. After the execution, a global evaluation function (*GEF*) is evaluated to decide whether to preserve the motion or roll it back. GEF incorporates all four parameters and is higher for better topologies. It is given by:

$$GEF = W1 * Connectivity + W2 * Coverage - W3 * Diameter$$

The obtained parameter values are normalized with respect to the desired values. Also, if a desired value for a parameter has been reached, its impact is de-emphasized by setting the weight for that parameter to zero. If a move is rolled back, a random perturbation of the nodes is employed followed by MSC-SNA or SNA singly. Note that rolling back is an artifice of the simulation used for this study and does not correspond to nodes retracing their path. The function can be calculated a priori before the motion is executed and the decision to execute the movement or not taken based on that. Also, the global state of the network cannot be known by any one node and therefore the GEF computation has to be approximated by considering a portion of the sensor field that is in a node's proximity. Alternatively, this task can be done at local cluster heads.

The efficacy of the MSC and the SNA algorithm has been theoretically proven. It has been shown that MSC causes all network nodes to converge to a single point if allowed to run indefinitely. The speed of convergence is along the path of steepest descent i.e. along the gradient. Thus it is an optimal choice for reducing the diameter of a network. The SNA algorithm has also been proven to be able to increase network coverage to the maximum possible value. Thus, sound theoretical foundations and ease of implementation make this intelligent motion algorithm a good choice for use in our study.

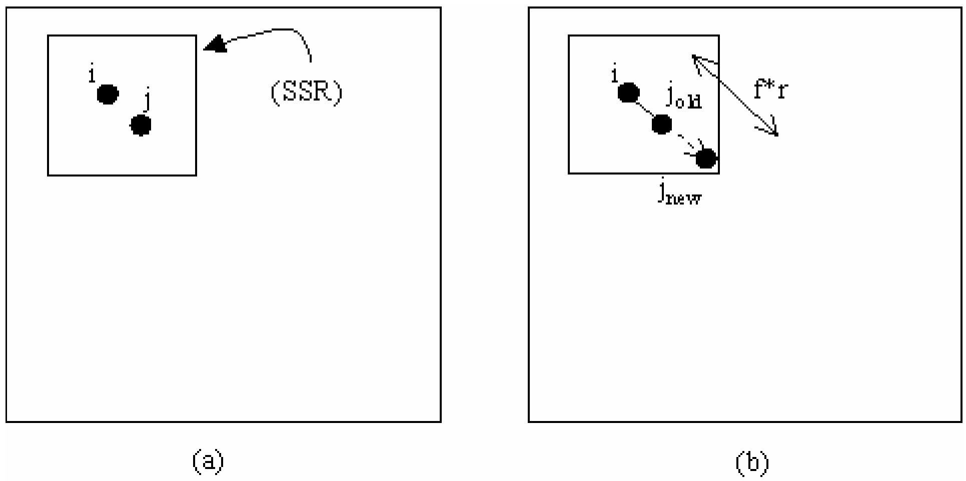

Fig. 3.2 SNA algorithm (a) current node position (b) node position after application of SNA

3.2 Robust Location Determination Protocol

The location determination protocol that we have used for this study is the Hop-Terrain and Refinement protocol of Saverese *et. al*. [7]. This two phase protocol is robust to errors in estimation of inter-node distances. The first phase of this algorithm involves running the Hop-Terrain protocol.

3.2.1 Hop-Terrain phase

In this phase the anchor nodes that have special location determination hardware broadcast *beacon* messages with their location coordinates. These messages have a *hop-count* field that indicates the number of hops traveled by the beacon message. This field is initially set to zero. Neighbors that receive these beacon messages increment the message’s hop-count field and further broadcast the message. Duplicate copies or copies from a previously seen anchor but a higher hop-count are dropped. This translates to a controlled flooding of the beacon messages. At the end of the hop-terrain phase all nodes in the system know their distance from the anchor nodes in terms of hops. In addition to this, the anchors also know the number of hops between them. As the distance between anchors is already known this can be used to estimate the average distance per hop. Based on this all nodes can calculate their approximate distance from the anchors. Using this distance and the knowledge of the location of the anchors, sensors can obtain an estimate of their location using error resilient triangulation. The hop-terrain phase does not use an exact distance estimate based on received signal strength at the nodes and instead uses the number of hops as a measure of distance. This is done because individual distance estimates can be erroneous and aggregation of these errors over multiple hops can lead to significant inaccuracies.

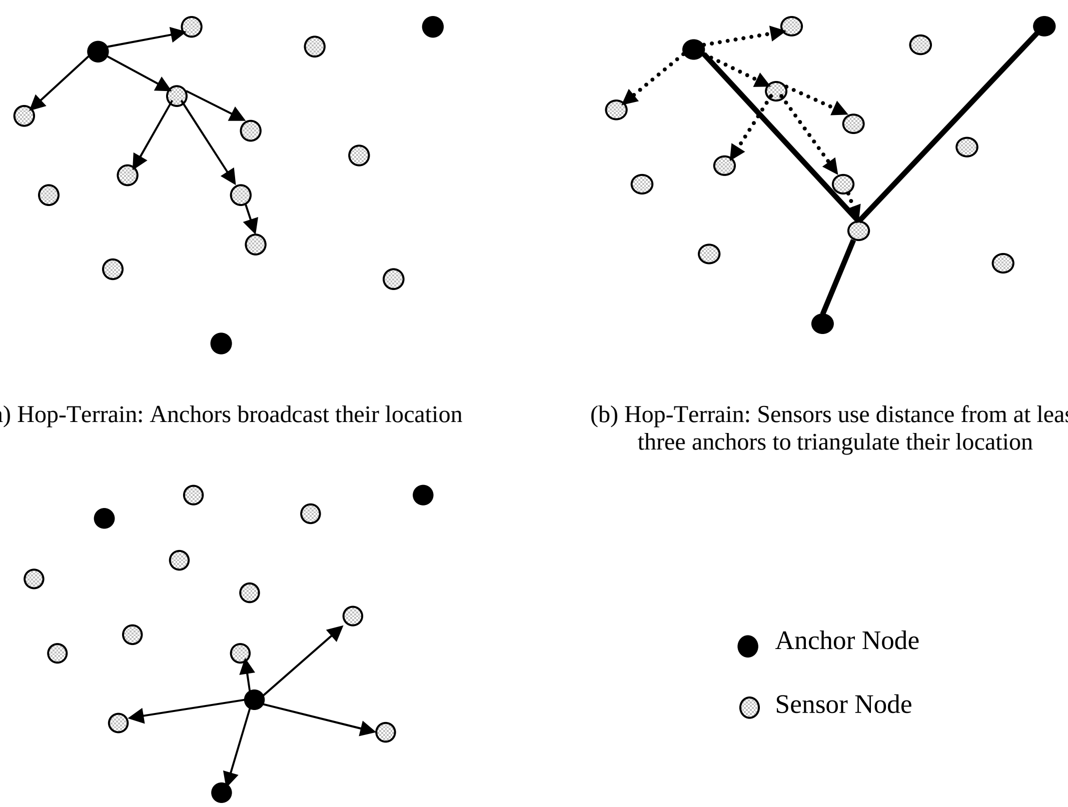

(a) Hop-Terrain: Anchors broadcast their location

(b) Hop-Terrain: Sensors use distance from at least three anchors to triangulate their location

(c) Refinement: Sensors with triangulated locations act as anchors and exchange location information with immediate neighbors

Fig. 3.3 Schematic of Hop-Terrain and Refinement Protocol

3.2.2 Refinement phase

The Hop-Terrain phase is only used to get an initial estimate of the location of sensor nodes. In the Refinement phase, all nodes behave as anchors and broadcast beacons containing their location coordinates obtained using Hop-Terrain. These beacons are not flooded and are only used by immediate (one hop) neighbors. The neighbors use received signal strength to estimate their distance from the source node of the beacon. This distance along with the location coordinates in the beacons is used to obtain a more refined estimate of the position of the sensor nodes using error resilient triangulation. This process is repeated with nodes transmitting beacons with their refined location coordinates until sufficiently accurate position estimates are obtained.

Two of the main challenges for a location determination protocol are low fraction of anchors in the network and large errors in inter-node distance estimates. The protocol being considered here is robust with respect to both of these problems. The error in the final position estimate made by the non-anchor nodes is the QoS metric of the protocol. The estimation error at a node is a function of the number of its one hop neighbors that have received the diffusion, called *neighbor connectivity*, and the number of anchor nodes from which the diffusion has been received, called *anchor connectivity.*

3.3 Experimental Evaluation

To evaluate the effect of topological characteristics of a network on the accuracy of location determination we conduct a simulation based study. We consider a set of network topologies and apply the intelligent motion model to them with different values of the desired topological characteristics. The Hop-Terrain and Refinement protocol is run on the resulting topologies and metrics indicating the accuracy of the location determination are collected. These are compared with the metrics obtained from the topologies generated by running the Random Way Point (RWP) motion model. In RWP a random destination is chosen for each node and it is moved to that destination with a random speed. This is a common model used for simulating uncontrolled or random node motion.

3.3.1 Simulation model

For the purpose of this study we use an event based simulator called the *network simulator-2* [31]. It is an open source simulator and was modified to support the Hop-Terrain and Refinement protocol. The sensor field used for the simulation was a two-dimensional rectangular grid with resolution *res*. The parameters used for the simulation are shown in Table 3.1.

Table 3.1
Parameters for simulation

Parameter	**Value**
Sensor field dimension	500m x 500m
Grid resolution	1m
Node transmission range	125m

3.3.2 Experimental results

The error in Hop-Terrain and Refinement is a function of the average number of neighbors of a node that have calculated their own locations based on their distance from at least 3 anchor nodes. The count of such neighbors for a node is called *neighbor connectivity*. Intuitively, neighbor connectivity can be improved by densely packing the nodes, but this comes at the expense of coverage. In the first experiment, we vary the number of sensor nodes, keeping the proportion of anchor nodes constant at 20%. We let the goal-driven motion achieve a coverage of 80% with a diameter of 6 and measure the neighbor connectivity. Similarly, the neighbor connectivity is measured after moving the nodes for the same amount of simulation time using RWP after which the neighbor connectivity is measured. Given neighbor connectivity, the error is looked up from [7].

Table 3.2 shows that using the intelligent motion model causes a definite improvement in the performance of location determination. This is a direct consequence of the ability of intelligent motion to pack the nodes in a uniform (high coverage) but dense manner (low diameter) causing the average neighbor connectivity to increase. Importantly, the relative improvement increases with increasing number of nodes. This is explained by the observation that the goal-directed motion is further capable of optimizing the topological characteristics with a larger number of nodes to place while RWP being random in nature cannot benefit from this. The goal-directed motion spreads nodes uniformly over the sensor field while RWP fails to achieve this. As a result, in the topology generated by goal-directed motion all nodes have a uniformly low error leading to an overall lower average error compared to RWP.

Table 3.2
Improvement in accuracy of location determination due to goal directed motion with varying number of nodes.

Number of Nodes	Random Motion		Goal-directed Motion (80% coverage, diameter=6)		Improvement (%)
	Neigh. Conn.	Error(%)	Neigh. Conn.	Error(%)	
30	5	22	11	12	45.5
40	6	20	14	8.5	57.5
50	7	18	17	7	61.1

Next, we show that the extent of improvement of the application QoS can be controlled for a given number of nodes by varying the topological characteristics that the goal-directed motion achieves. The results with the number of nodes kept constant at 30 are shown in Table 3.3. Expectedly, the improvement is most marked when the mobility algorithms achieve low diameter. However, a network designer can constrain the allowable coverage and use the motion algorithms to achieve different QoS improvements. These results are especially noteworthy because they show how QoS of one application can be traded for another. For example, if a surveillance application demands that at least 80% of the sensor field be covered by the sensors then at least 12% error in the calculated location coordinates of the sensors will have to be tolerated. This corresponds to the minimum achievable diameter corresponding to 30 nodes and 80% coverage as derived from the intelligent mobility algorithm.

Table 3.3
Different topological characteristics and corresponding improvements in location determination using goal-directed motion (number of nodes = 30)

Coverage	Diameter	Neigh. Conn.	Error(%)	Improvement (%)
Random Way Point		5	22	NA
55	4	16	7	68.1
62	6	15	8	63.6
70	6	13	9	59.1
80	6	11	12	45.5
80	8	9.5	13	41

The simulation model used for obtaining the above results is generic and can be used for designing any practical network. More importantly, it can be used for motion planning in scenarios where controlled mobility is possible. One such instance is a scenario where the nodes are deployed quickly in dense clusters and then diffuse to different regions of the sensor field for their operation. This includes scenarios where sensor nodes are fitted in the combat kits of soldiers of a special forces unit and their squadron is deployed in a hostile urban environment. Another example is sensor nodes being fitted on robots sent in for an emergency clean up of a toxic chemical leak in a factory building. In both these situations sensors are likely to be initially deployed close to building entrances. Our simulation model can be applied in such situations to suggest positions the soldiers or robots should try to take after they have been initially deployed in small clusters near the entrances. This can help ensure that they adequately cover the hostile territory (coverage) and do not get separated (connectivity) or go too far from each other (diameter) while at the same time giving their commanders the ability to monitor their positions and location of origin of their sensory data with sufficient accuracy.

4. LOCATION DETERMINATION WITH DIRECTIONAL ANTENNAS

Received signal strength based range estimation is a widely applicable technique for calculating inter-node distances in a sensor network. This is in part caused by the physical limitations of other techniques such as those based on the time of flight. In addition to this, RF transceivers are already part of the sensor nodes for communication purposes. Measuring the strength of received RF signals requires minimum additional hardware. The range estimates can be obtained from communication messages that are part of other application level protocols and this saves the expenditure of energy in transmission of special range estimation beacons.

Received signal strength has traditionally been used in systems that are equipped with omni-directional antennas for communication. For such systems the received power at a distance r from the transmitter can be modeled with a reasonable accuracy as

$$P_r = \frac{P_t}{r^k} \tag{4.1}$$

where P_r is the received power, P_t is the transmitted power and k is a model parameter. For outdoor environments with *line of sight* communication a choice of k equal to 2 gives a fairly accurate model of the system. As is obvious from equation (4.1), r can be easily estimated by measuring P_r if the value of P_t is known from prior calibration of the system. Even though the range estimates thus obtained have errors, use of robust positioning algorithms such as Hop-Terrain and Refinement can give fairly accurate location estimates.

The problem of range estimation using received signal strength becomes challenging when directional antennas are used on sensor nodes. To understand the problem let us assume a relatively simple cosine model for the directional gain of an antenna. The directional gain of an antenna is the factor that controls the amount of power that is radiated in a particular direction by the antenna. So, the transmitted power in a direction making an angle θ with the antenna axis is given by equation (4.2)

$$P(\theta) = P_t.\cos(\theta) \tag{4.2}$$

If the receiving antenna has a similar gain then the received power at a distance *r* is given by

$$P_r = \frac{P_t}{r^k}.\cos(\theta_t).\cos(\vartheta_r) \tag{4.3}$$

where θ_t and θ_r are the transmission and receiving angles respectively. This equation has a total of three unknowns i.e. *r*, θ_t and θ_r. Thus, estimation of inter-node distances by measurement of received signal strength is non-trivial. In the rest of this section we present a set of techniques that can be used for range estimation using received signal strength for systems deploying directional antennas. We also present simulation results that demonstrate the efficacy of the proposed technique and its robustness to errors.

4.1 Directional Antenna Model

One of the simplest semi-directional antennas is the patch antenna. This antenna is used as a representative example of an antenna that may be used for localization and that will still fit on the small form-factor of a sensor node. The ideal patch radiation model is a hemispherical radiator that allows for semi-directional radiation. The typical gain of a patch antenna is of the order of 3.5 dBm to 6 dBm depending on the dielectric substrate used in the design. The angular variation of the gain *G(θ)* for a typical microstrip antenna is in the range of $\cos^2\left(\frac{\beta\ell}{2}\sin(\theta)\right) < G(\theta) < \cos\left(\frac{\beta\ell}{2}\sin(\theta)\right)$ where β is the free-space phase constant and *l* is the length of patch [32].

In the E-plane cut, the electric field intensity from a standard patch radiator is given by

$$E(\theta) = E_0\cos\left(\frac{\beta\ell}{2}\sin(\theta)\right) \tag{4.4}$$

This is the radiation pattern in a plane along the normal to the radiating surface of a microstrip patch antenna. In Fig. 4.1, the radiating surface of antenna 1 is in the yzplane and the normal to the antenna is along the x-axis. Equation (4.4) gives the pattern of variation of electric field intensity in the xy-plane for a direction making an angle θ with the x-axis. This is the pattern for a constant z-coordinate value i.e. at a fixed elevation from ground. This is the ideal pattern for a patch antenna with an infinite ground plane that is only slightly altered when using a finite size ground plane. The ground plane is used to shield the radiating field from the rest of the circuitry and other radiators. A patch antenna is, therefore, less sensitive to parasitic radiators that effect many omni-directional antenna designs.

The received power at an antenna is given by $P_r = {}^{P_t}\!/_{r^2}\, G(\theta_t)H(\theta_r)$ where θ_t and θ_r are the transmitting and the receiving angles, respectively and r is the distance between the transmitter and the receiver.

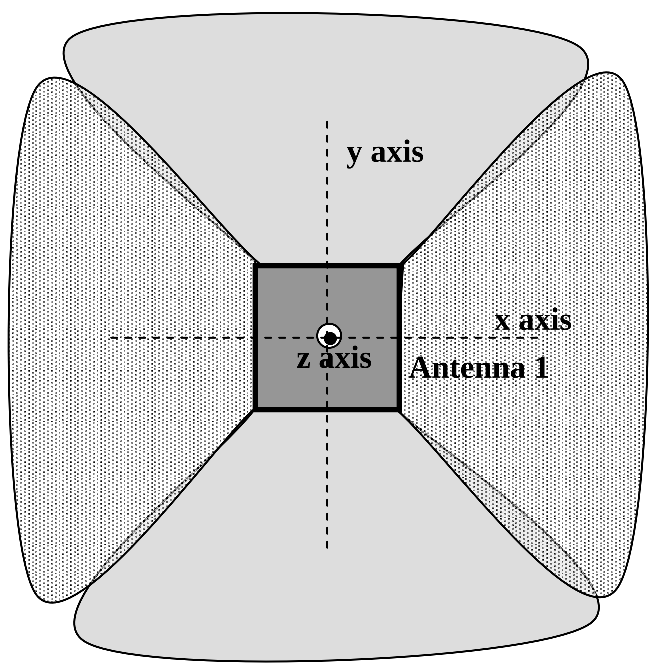

Fig. 4.1 Deployment of directional antennas

For the purpose of this work we use an antenna model given by $G(\theta) = H(\theta) = \cos^2\left(\frac{\beta\ell}{2}\sin(\theta)\right)$. This corresponds to the square of the factor used for modeling the directional gain of the electric field intensity. However, the proposed techniques are also valid for some other single lobe antenna radiation models such as $P(\theta) = P_t . \cos(\theta)$. The schemes proposed in this thesis work if the transmitting lobes of multiple antennas on a node intersect at a unique point as shown in Fig. 4.2(b)

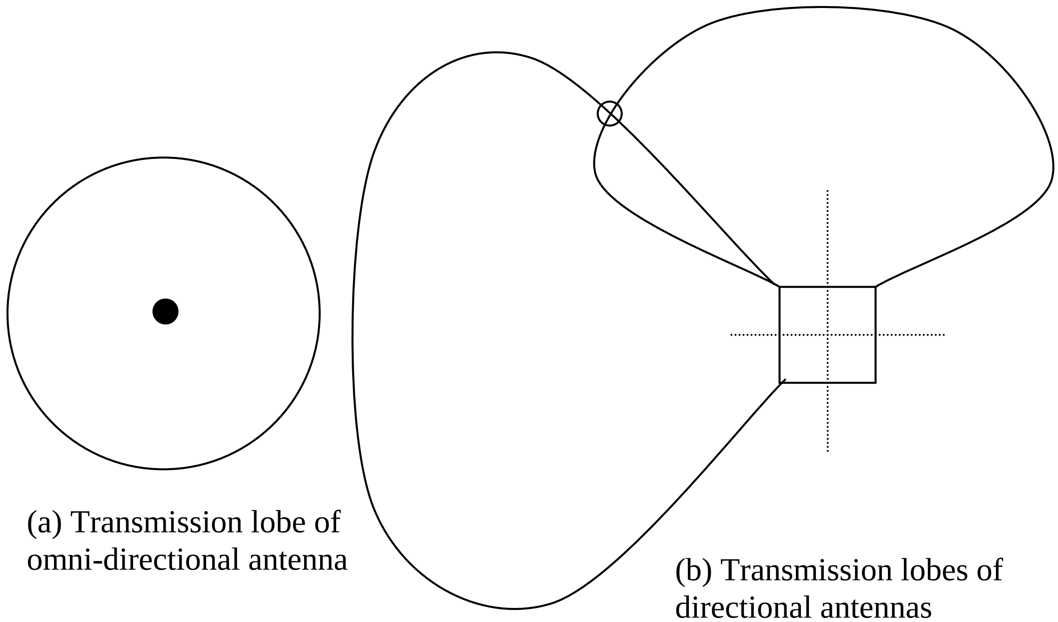

Fig. 4.2 Transmission lobes on antennas

Directional antennas are usually deployed in a diversity configuration on sensor nodes. For this thesis, we assume that four such antennas are deployed one along each of the four sides of a square representing a sensor node. Fig. 4.1 shows such an arrangement with four lobes representing the radiation fields of the antennas. Together these four antennas cover the entire 360˚ (2B) sensor field. To restrict the location determination problem to a two-dimensional plane, we assume that all antennas are at the same height from the ground.

4.2 Range Estimation with Directional Antennas

Having chosen an appropriate model to represent the received signal strength for directional antennas, we proceed with a formulation of the solution to the range estimation problem. We study the problem for different kinds of node deployments ranging from stringent requirements on node alignment to a completely general solution.

4.2.1 Aligned antennas

In a number of practical applications it is reasonable to expect that the sensors will be manually deployed. For instance, sensors set up to monitor a bridge's structural health will have to be manually placed by construction workers on the bridge. In such scenarios even though it may not be possible to know the precise location of the sensor, it is possible to place these sensors in a pre-determined orientation. For instance, construction workers may be instructed to place sensors using a magnetic compass so that they are always aligned in the north-south direction. It should be noted that in such a scenario the accuracy of node alignment is affected by non-uniformity of the earth's magnetic field. Local phenomena such as the effect of power transmission lines or large iron structures may have to be accounted for while deploying nodes. It may be argued that the locations of the sensors can also be fed in to the nodes during manual deployment. For a mobile network these initial locations will be meaningless and periodic updates of location through a location determination protocol will still be required. Moreover, hardware used for global alignment such a magnetic compass is both cheaper and smaller than a GPS receiver. This means that while it may not be possible to equip all sensor nodes with special location determination hardware, it may still be possible to equip all the nodes with affordable alignment hardware.

If the antennas of nodes are aligned, then location estimation can be performed by measuring the power received at multiple receiving antennas on a sensor node from a single transmitter on an anchor. Without loss of generality consider that an anchor node is placed to the south-east of the sensor node as shown in Fig. 4.3.

From this figure,

$$\Theta_{t2} - \Theta_{t1} = \Theta_c$$

$$\Theta_{t1} = \frac{\pi}{2} - \Theta_1$$

$$\Theta_{t2} = \Theta_2$$

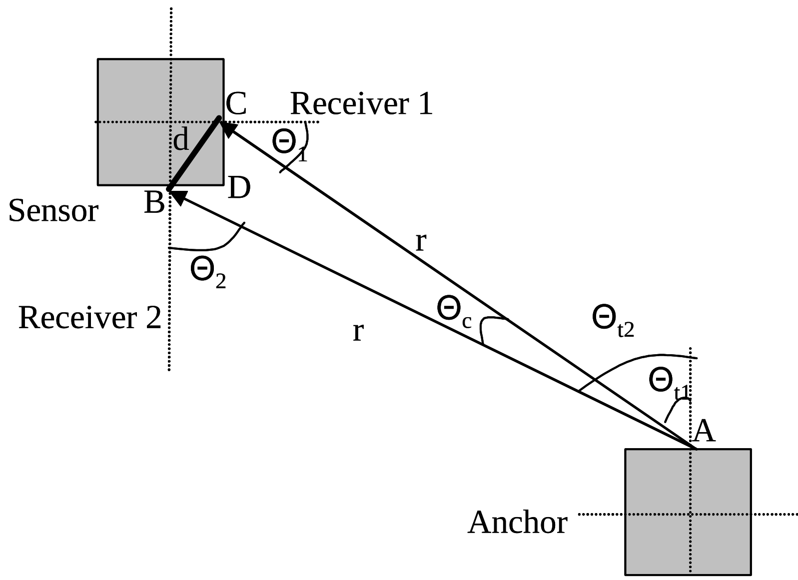

Fig. 4.3 Location determination with aligned nodes

Typically, the size of the sensor node would be much smaller than the inter-node distance. So, the distance between the centers of adjacent antennas *d<<r*. In such a situation it is reasonable to assume that the propagation path for signals to both the receiving antennas is approximately of the same length *r*. Thus, $\Theta_c = d/r$.

The received power at the two sensor antennas is given by

$$P_{r1} = \frac{P_t}{r^2} G(\Theta_{t1}) H(\Theta_1) = \frac{P_t}{r^2} G(\frac{\pi}{2} - \Theta_1) H(\Theta_1) \quad (4.5)$$

$$P_{r2} = \frac{P_t}{r^2} G(\Theta_{t2}) H(\Theta_2) = \frac{P_t}{r^2} G(\Theta_2) H(\Theta_2)$$

$$\Rightarrow \mathrm{P}_{r2} = \frac{P_t}{r^2} G(\frac{\pi}{2} + \frac{d}{r} - \Theta_1) H(\frac{\pi}{2} + \frac{d}{r} - \Theta_1) \quad (4.6)$$

Thus, we have two equations (4.5) and (4.6)in two variables Θ_1 and *r*. As these are nonlinear equations, it is difficult to get a closed form solution for Θ_1 and *r* in terms of the input variables P_{r1} and P_{r2}. However, these equations can be numerically solved by standard methods to obtain Θ_1 and *r*.

The solution of the system of equations gives the distance as well as the relative direction of the sensor with respect to the anchor node. Thus, the position of the sensor node can be estimated by vector addition as shown in Fig. 4.4. This estimate is based on measurements from only one neighboring anchor node whereas location determination using omni-directional antennas requires measurements from at least three anchors. Moreover, an estimate of the position of the sensor can be obtained by the transmission of only one message by the anchor node. Techniques that use omni-directional antennas require three message transmissions for obtaining an estimate of the position of the sensor node. Since message transmissions are one of the main sources of energy consumption in a sensor network, the proposed technique can be used to enhance the battery life of sensor nodes.

By using directional antennas, estimates from multiple anchors can be averaged to obtain a better estimate of the position. Alternatively, the information about Θ_1 can be discarded and the range measurements (r) can be used to triangulate the position of the sensor in a least squares manner as described in section 2.2. Both these strategies have been evaluated in our simulations.

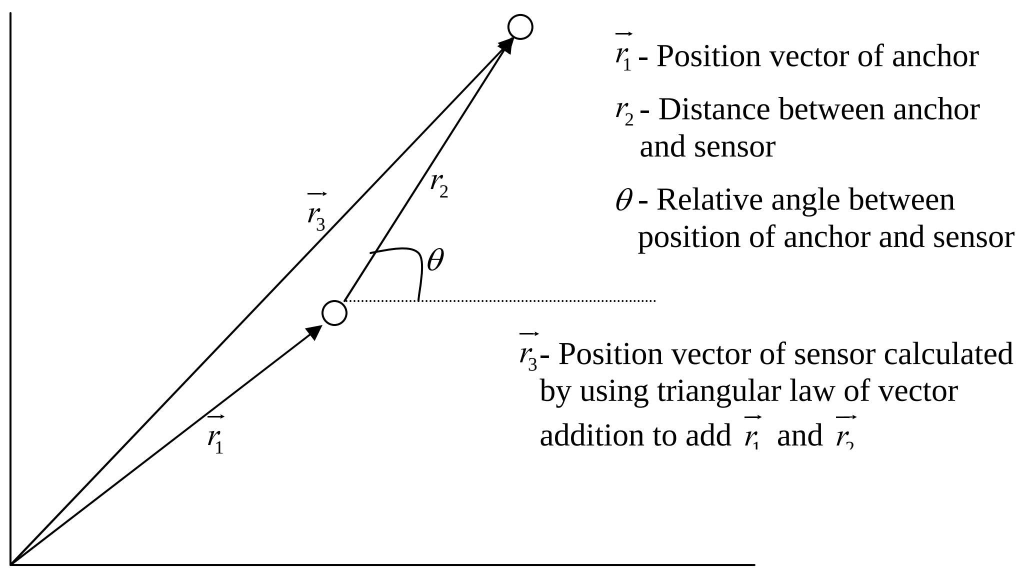

Fig. 4.4 Vector addition to obtain location coordinates of sensor node

4.2.2 General antenna orientation

In situations where it is not possible to ensure a global orientation for all nodes of a network, additional measurements can be used to estimate position of sensor nodes. Received power at two different antennas on the sensor node from two transmitting antennas on the anchor node needs to be measured. Such an arrangement is shown in Fig. 4.5. Geometric relations between the various transmission and receiving angles can be derived from Fig. 4.5.

$$\Theta_2 + \Theta_6 = \Theta_4 + \Theta_8 = \Theta_3 + \Theta_5 = \Theta_1 + \Theta_7 = \frac{\pi}{2} + \frac{d}{r}$$

$$\Theta_1 + \Theta_2 + \Theta_3 + \Theta_4 = \pi$$

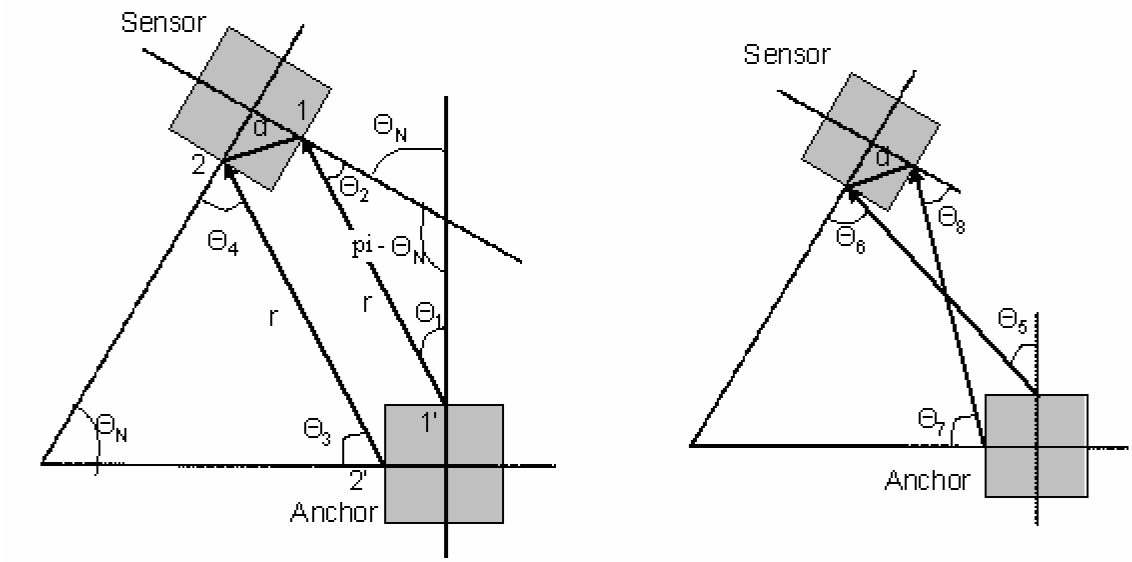

Fig. 4.5 Location determination with unaligned antennas

Let P_{rij} denote the power received by antenna i on the sensor node when antenna j on the anchor node is transmitting. We can use these equations to simplify the received power equations as follows

$$P_{r11'} = \frac{P_t}{r^2} \cdot G\left(\pi - \Theta_2 - \Theta_3 - \Theta_4\right) \cdot H\left(\Theta_2\right) \tag{4.7}$$

$$P_{r21'} = \frac{P_t}{r^2} \cdot G\left(\frac{\pi}{2} + \frac{d}{2}\pi - \Theta_3\right) \cdot H\left(\frac{\pi}{2} + \frac{d}{2} - \Theta_2\right) \tag{4.8}$$

$$P_{r12'} = \frac{P_t}{r^2} \cdot G\left(\frac{d}{r} + \Theta_2 + \Theta_3 + \Theta_4 - \frac{\pi}{2}\right) \cdot H\left(\frac{\pi}{2} + \frac{d}{r} - \Theta_4\right) \tag{4.9}$$

$$P_{r22'} = \frac{P_t}{r^2} \cdot G\left(\Theta_3\right) \cdot H\left(\Theta_4\right) \tag{4.10}$$

Equations (4.7), (4.8), (4.9) and (4.10) in the four variables Θ_2, Θ_3, Θ_4, and r can again be numerically solved to estimate the location of the sensor node.

This scheme requires that two sensor antennas be able to simultaneously receive transmissions from two anchor antennas. This would require a transmitter beam width of 180˚(B). This is non-optimal for four antennas covering a 360˚(2B) plane but is a tradeoff for increased degrees of freedom in the orientation of the nodes. Besides, the increased beam-width may sometimes be desirable. It increases the fault tolerance of the system by providing redundancy in the spatial reach of the antennas. It will also ease the constraints on antenna design since high directionality i.e. narrow beam width is not needed. This makes directional antennas cheaper to manufacture.

This scheme requires two message transmissions by the anchor node for obtaining an estimate of the position of the sensor node. This is an improvement over three message transmissions required by omni-directional antenna based techniques and can lead to energy conservation in a sensor network.

4.2.3 Aligned antennas with two anchors

The location determination methods described earlier rely on the difference in power received at two antennas on a sensor node. This received power corresponds to the same signal emanating from an antenna on an anchor. If the distance between the receiving antennas is of the order of the carrier wavelength, then the two propagation paths from the transmitter to the receiving antennas are approximately the same. Environmental factors and other noise in the transmission channel now affect both the received signals in similar ways. This leads to correlated errors in the received power measured at the two antennas. Our model for the received power at an antenna does not consider correlated errors. However, in a real life scenario this can adversely affect the accuracy of location estimation. A typical carrier frequency of 900 MHz restricts the use of the methods outlined in the two previous sections (4.2.1, 4.2.2) to diversity antennas mounted on equipment at least the size of a notebook computer. In spite of a restriction on node size, these techniques are still useful for a large number of applications, such as determining the location of production equipment and maintenance workers on the factory floor in an intelligent factory [33]. However, a different scheme is needed for handling smaller sized nodes, such as smart dust sensor nodes [2].

To achieve this, the location determination scheme for aligned antennas can be modified to use power measurements from two anchors. The arrangement is shown in Fig. 4.6

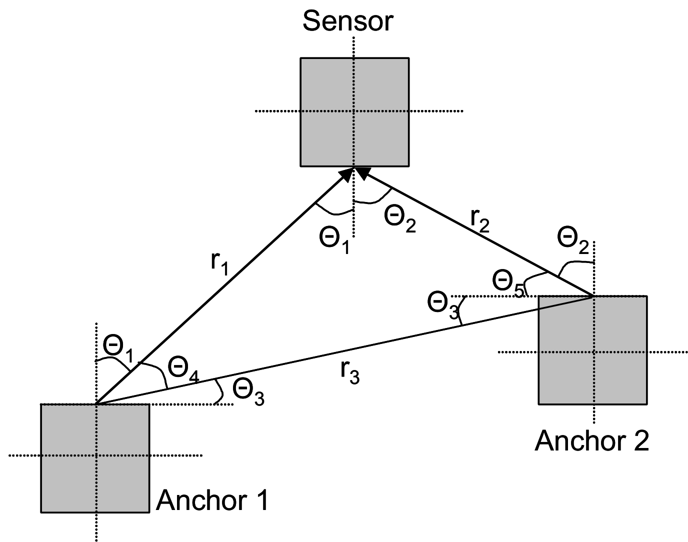

Fig. 4.6 Location determination using measurements from two anchors

As the location of the two anchors is known, the parameters r_3 and Θ_3 can be determined. Let the coordinates of anchors 1 and 2 be (x_1,y_1) and (x_2,y_2) respectively. Then

$$r_3 = \sqrt{(x_2 - x_1)^2 + (y_2 - y_1)^2}$$

$$\Theta_3 = \tan^{-1}\left(\frac{|y_2 - y_1|}{|x_2 - x_1|}\right)$$

Using geometrical properties of the system we get the following relations between the various angles

$$\Theta_5 = \frac{\pi}{2} - \Theta_2$$

$$\Theta_1 + \Theta_3 + \Theta_4 = \frac{\pi}{2}$$

The equations for the received power are given by

$$P_{r1} = \frac{P_t}{r^2} \cdot G(\Theta_1) \cdot H(\Theta_1) \tag{4.11}$$

$$P_{r2} = \frac{P_t}{r^2} \cdot G\left(\Theta_2\right) H\left(\Theta_2\right) \tag{4.12}$$

Using the sine law of a triangle along with relations between the angles derived earlier we get two more equations

$$\frac{r_2}{\cos\left(\Theta_1 + \Theta_3\right)} = \frac{r_3}{\sin\left(\Theta_1 + \Theta_2\right)} \tag{4.13}$$

$$\frac{r_1}{\cos\left(\Theta_2 - \Theta_3\right)} = \frac{r_3}{\sin\left(\Theta_1 + \Theta_2\right)} \tag{4.14}$$

This gives us four equations in the four unknowns r_1, r_2, Θ_1, and Θ_2, which can be solved numerically. Thus, the distance of the sensor from the anchors and the relative angle of its position with respect to each of the two anchors can be determined. The sensor node's location can be estimated using either of the (distance, angle) pairs.

In this section, we have provided a mathematical solution to the problem of location estimation with directional antennas in three different scenarios. In practice, the node specifications and the deployment conditions will determine which scenario is applicable.

4.3 Analysis of Error in Location Estimation

In this section, we provide an analytic estimate of the error in location estimation in a two-dimensional plane using the triangulation approach. The analysis brings out the relation between error and the number of neighboring anchor nodes with respect to which triangulation is performed. For the purpose of this analysis, we assume a model in which triangulation is done with distinct sets of three anchor nodes to determine the sensor node's location. After this an averaging is performed over all the location estimates to obtain a final estimate of the sensor's location. This method is somewhat different from the error resilient triangulation technique and is only used to facilitate this analysis. Least square estimation is known to give an optimal solution in the presence of Gaussian errors. Hence the expression for error obtained by this analysis will give an upper bound on the error in estimation using triangulation.

First, consider a set S1 with three anchor nodes whose location coordinates are (x_1, y_1), (x_2, y_2), (x_3, y_3). The location of the target node that is to be determined is (u_x, u_y). Let the distances measured from the three neighbors be r_1, r_2, and r_3. These distances are estimated from the received signal strength measurements and can be erroneous. We set up three distance equations with respect to the three neighbors as follows

$$\left(x_1 - u_x\right)^2 + \left(y_1 - u_y\right)^2 = r_1^2 \tag{4.15}$$

$$\left(x_2 - u_x\right)^2 + \left(y_2 - u_y\right)^2 = r_2^2 \tag{4.16}$$

$$\left(x_3 - u_x\right)^2 + \left(y_3 - u_y\right)^2 = r_3^2 \tag{4.17}$$

Solving equations (4.15) - (4.17), we get u_x to be of the following form.

$$u_x = k_1 r_1^2 + k_2 r_2^2 + k_3 r_3^2 + k_4 \tag{4.18}$$

Here $k_i \in R$ i.e. k_i are real numbers whose values depend only on the location of the three anchors and are independent of values r_i The value of u_y can also be expressed in a form similar to that given by equation (4.18). One simple relation for measuring error in u_x and u_y is to differentiate both sides of the equation which gives

$$\Delta u_x = 2k_1 r_1 \Delta r_1 + 2k_2 r_2 \Delta r_2 + 2k_3 r_3 \Delta r_3$$

However, this is dependent on topology and no obvious bounds exist for the error. We choose to work with variances as a measure of the error in location estimation. Variance of data gives an estimate of the average of the squared error. The range measurements are error prone, and this leads to the error in location estimation of the sensing node. If we assume that the errors in range measurements are uncorrelated, then from equation (4.18), we get the variance of the estimated location to be of the following form.

$$\operatorname{var}\left(u_x\right) = k_1^2 \operatorname{var}\left(r_1^2\right) + k_2^2 \operatorname{var}\left(r_2^2\right) + k_3^2 \operatorname{var}\left(r_3^2\right) \tag{4.19}$$

The cross terms of the form $2k_ik_j$. E[(r_i^2 - E[r_i^2]) . (r_j^2 – E[r_j^2])] in the above expression are zero because of the assumption that the distances and their squares have uncorrelated errors. The range estimates are obtained at different times from different anchors. The transient electromagnetic phenomenon in the transmission channel that caused errors in range estimation are fairly dynamic. So, the assumption about uncorrelated errors is valid in practice.

For simplicity, consider that the number of neighbors N is divisible by 3. This can be used to construct $N/3$ sets of three equations each of which gives a value for (u_x, u_y). Each of these can be regarded as a sample value of a random variable. Therefore, the number of sample values of u_x and u_y is $p = N/3$. To maintain the independence of the samples it is important to have sets of three distinct equations and not to use an equation from one set in any other set. This results in the number of samples being $N/3$ and not ${}^{N}C_{3}$. The expected value of the calculated location is the sample mean, which is the same as the expected value of the population mean. Thus, this technique gives an unbiased estimate of the location. The variance of the final estimate of the location is given by

$$\mathrm{var}\left(u_{xp}\right) = \frac{\mathrm{var}\left(u_x\right)}{p}$$

The variance $var(u_{xp})$ is actually the *ensemble variance* while the variance computed in equation (4.19) is the *time variance*. To understand this better, consider that all measurements of range vector $[r_1, r_2, r_3]$ represent a stochastic process $[r_1(s,t), r_2(s,t), r_3(s,t)]$ where s is the space parameter and t is the time parameter. The variance in (4.19) is computed from samples obtained from a fixed set of three neighbors so the value of s is constant. The variance in $[r_1, r_2, r_3]$ is from the difference in values of this vector depending on the time at which the measurements are made. So the averaging is over time and hence the computed variance is a time variance. Unlike this, while averaging over $N/3$ sets of neighbors; we are averaging over different samples obtained at the same time slice of the stochastic process. This averaging when done over these multiple sample paths constitutes the ensemble average. If we assume ergodicity of mean and variance then the time average and variance can be replaced by the ensemble average and variance that we need for the subsequent analysis.

Chebyshev's inequality gives that for a random variable X with a distribution having finite mean μ and finite variance σ^2, $P(|X-\mu| \geq t) \leq \sigma^2/t^2$ for $t \geq 0$. Applying this to the random variable u_{xp}, we get the probability of the error in location estimation $|u_{xp} - E[u_{xp}]|$ exceeding a given error bound ε (in distance units) as follows

$$P\left(\left|u_{xp}-E\left(u_{xp}\right)\right|\geq\varepsilon\right)\leq\frac{1}{\varepsilon^2}\operatorname{var}\left(u_{xp}\right)$$
$$P\left(\left|u_{xp}-E\left(u_{xp}\right)\right|\geq\varepsilon\right)\leq\frac{1}{p\cdot\varepsilon^2}\operatorname{var}\left(u_x\right) \quad (4.20)$$

Equation (4.20) gives a bound on the probability of error in terms of the number of neighbors. Given a desired accuracy, we can make the probability of error exceeding the desired accuracy to be as small as we like by increasing *p*, i.e., by extension, increasing the number of neighbors *N*. Next, we have to determine the variance in u_x to complete the analysis. In equation (4.19), if we take the errors in the three range measurements r_1, r_2 and r_3 to be equal, then the variance in u_x can be written as follows

$$\operatorname{var}\left(u_x\right)=\left(k_1^2+k_2^2+k_3^2\right)\cdot\operatorname{var}\left(r^2\right) \quad (4.21)$$

In general, the coefficients k_1, k_2, k_3 are dependent on topology, i.e., the relative placements of the neighbors with respect to the sensing node. The upper bound for the sum is infinity (when the three neighbors are collinear) and the lower bound is achieved when the triangles formed by the neighbors with the sensing node are equilateral [15]. We run MATLAB simulations with varying placements of neighboring nodes in the topology shown in Fig. 4.7. For values of the angle θ subtended by the neighbors at the target node between ${}^{5}\!/_{36}\,\pi\left(25°\right)$ and ${}^{1}\!/_{3}\,\pi\left(60°\right)$, it is seen that $\left(k_1^2+k_2^2+k_3^2\right)$ lies close to ${}^{0.2}\!/_{R}$ where *R* is the distance between the neighbor and the target node.

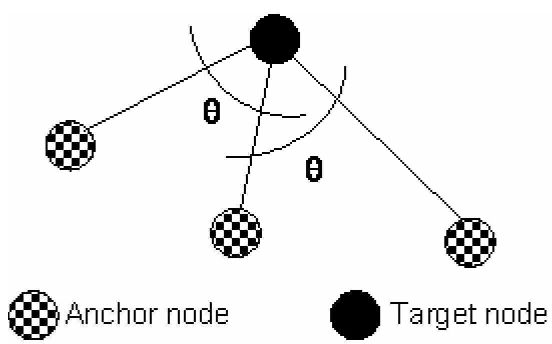

Fig. 4.7 Topology of anchor and sensor nodes

Next, we compute the variance in r^2. Let the upper bound on the relative error in distance measurements be *e*. This means that if the actual distance between an anchor node and the target node is *r*, the measurement lies between ($r \pm e.r$). Assume that the distance measurements follow a Gaussian distribution. Therefore, almost all the points (99.74% to be exact) lie within ($r \pm 3\sigma$). Equating, $\sigma = {e.r}/{3} \le {er_T}/{3}$, where er_T is the threshold on the maximum tolerable error in range estimates. Thus, $\mathrm{var}(r) \le \left({er_T}/{3} \right)^2$. Next, to calculate $var(r^2)$ we observe that $var(r^2)$ = E[r^4] – (E[r^2])^2. The higher order expectations can be calculated using the *Moment Generating Function* (MGF). MGF of a Gaussian distribution with mean μ and variance σ^2 is $M(t) = e^{\left(\mu t + \frac{\sigma^2 t^2}{2}\right)}$. E[$r^2$] and E[$r^4$] can be derived by differentiating $M(t)$ twice and four times, respectively, and evaluating it at $t = 0$. Simplifying and using equations (4.20) and (4.21), the probability of the error in location on the x-axis exceeding a given bound ε is as follows.

$$P\left(\left|u_{xp} - E\left[u_{xp}\right]\right| \ge \varepsilon\right) \le \frac{1}{p \cdot \varepsilon^2} \cdot (0.2) \cdot e^2 \cdot R^3 \left(\frac{2}{81} e^2 + \frac{4}{9}\right) \qquad (4.22)$$

This formula shows that location estimation over short distances is much more accurate because there is a cubic term in R, the distance between the anchor node and the target node. Consider some sample values for the different parameters: Tolerable error in location in one axis ε = *1 m*, distance between anchor and sensor node R = *5 m*, relative error in individual measurement e = *5%*. Suppose, we want to have less than 1% probability that the aggregate error in location estimation exceeds the threshold ε. Then, equation (4.22) gives that p ≥2.7754. As N=3p, the number of anchor node neighbors ≥ 8.33. This implies there must be at least 9 neighbors of the sensor node for a tolerable error. Note that the equation is identical in any dimension and therefore the calculated number of neighbors is also going to bound the error in the other axes by the same amount. If more accurate location estimation is desired in some axis, then the one with the most stringent accuracy requirement will determine the number of neighbors needed.

A similar analysis cannot be performed for the directional antenna methods proposed in section 4.2. This is because a closed form solution for the location of sensor nodes in terms of power measurements cannot be derived. We compare the aggregate error in the directional antenna approach to the triangulation approach through our simulation experiments that are detailed in section 4.4.

4.4 Experiments and Results

To evaluate the efficacy of the proposed set of location determination schemes, a simulation of the methodology was carried out in MATLAB. The goal of the experiments was to evaluate the robustness of the proposed schemes to errors in received signal strength. These errors, which are a measure of the deviation of received signal strength observed in practice from the values predicted by the antenna model, can be a result of factors such as channel noise, multipath fading, obstacles in the environment or even the lack of an appropriate antenna radiation model. We consider random placements of a sensor and neighboring anchors in a sensor field. The received power at the sensor from neighboring anchors under ideal conditions i.e. in the absence of any errors is calculated. This is perturbed by a random error and the erroneous power values are used for estimating the position of the sensor node. The choice of an appropriate error model for the received signal strength is not clear. For *line of sight* communication the error in the envelope of received signal is modeled by a *ricean distribution*. For *non line of sight* communication the corresponding model is the *rayleigh distribution*. The instantaneous value of the received signal strength is proportional to the square of the instantaneous value of the signal envelope. Thus, the error in the instantaneous signal strength for both these models follows a *chi-square distribution*. But the signal strength used for location determination is the average of the received signal strength over a small time window. So, use of a chi-square distribution to model errors in it would be incorrect. In the absence of a model based on more concrete physical properties of the system we choose a *normal distribution* to model errors in received power. Due to the *central limit theorem* a Gaussian distribution can be used to adequately represent random phenomenon resulting from the cumulative effect of a large number of independent and identically distributed random processes. As the error in received power is also the result of a combination of factors such as multipath fading, environmental conditions, thermal noise etc. it is reasonable to model it with a Gaussian distribution. We also report results for a uniform distribution of errors. The general trends observed with a uniform distribution of errors are similar to those observed with normal distribution of errors. The distance between the estimated position of the sensor in the simulation and its true position gives us a measure of error in location determination. To remove the effect of scale all the location estimation error values reported in this section have been expressed as a percentage of the transmission range of the sensor nodes.

Three different scenarios discussed in Sections 4.2.1, 4.2.2 and 4.2.3 have been simulated – aligned antennas with single anchor (one Align), general i.e. possibly unaligned, orientation of antennas with single anchor (one Gen), and aligned antennas with two anchors (two Align). In all these schemes estimates of the location of sensor nodes are obtained from multiple neighboring anchor nodes. These location estimates are averaged to obtain the coordinates of the location of the sensor node. One Align LSE refers to Least Square Estimation which is based on the error resilient triangulation technique. In this scheme the position of the target sensor node is estimated using the aligned antenna technique described in section 4.2.1. This provides both the distance and relative angle between the anchor and the sensor. For one Align LSE scheme the angle information is discarded and the range estimates are used to set up a system of equations for error resilient triangulation. The one Gen LSE scheme is a similar derivation of the scheme developed in section 4.2.2 for use with ERT. The five schemes are compared to the ERT scheme with omni-directional antennas (Omnidirectional).

The methodology used for conducting these simulations involves placing a sensor node in a two dimensional sensor field. Anchor nodes are placed at random locations around this sensor node in the sensor field. The exact number of neighboring anchors is a simulation parameter. The power expected to be received by the sensor from the neighboring anchors is calculated. This is perturbed by a normal random variable whose variance is another simulation parameter. This variance value has been reported as a measure of the error in received power as it is the deviation in actual received power from the value predicted by the antenna radiation model. Based on the erroneous values of received power the position of the sensor node is calculated. Two error checks have also introduced in the system. The first error checking mechanism discards location estimates which predict the distance between the sensor and the anchor node to be greater than the transmission range of the anchor nodes. The second error checking mechanism ensures that the estimated position of the sensor node puts it in the same quadrant with respect to the anchor node as was used for solving the system of equations for location determination. Because of the random nature of the error model these error checks can bias results by selectively discarding samples with large error values. To avoid this, the error values are generated at the beginning of the simulation. The location estimates that do not pass the error checking are recalculated for the same value of random error but a different location of the anchor node.

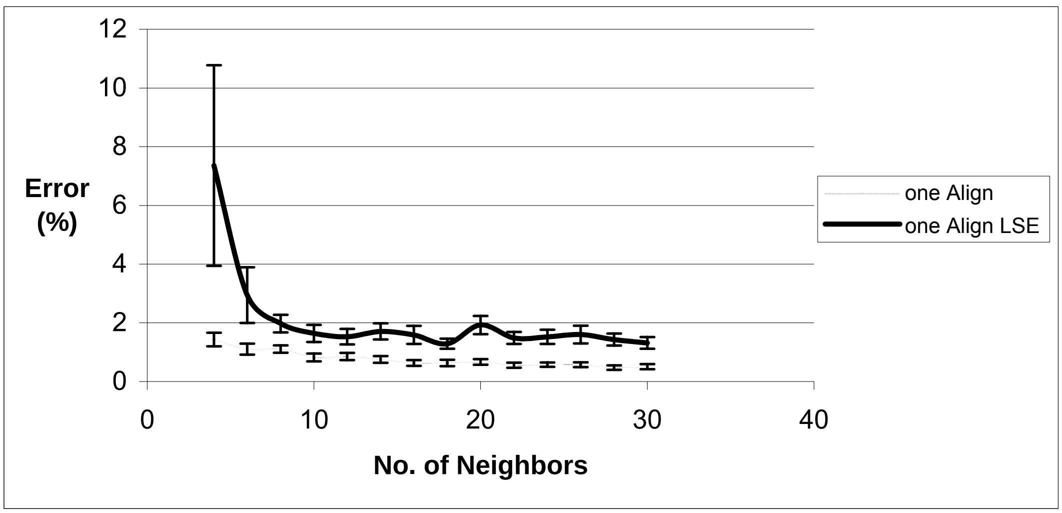

Fig. 4.8 Comparision of error resilient triangulation with averaging for directional antennas

Fig. 4.8 shows the error in position estimation as a percent of the transmission range. The error is expressed as a function of the number of neighboring anchors from which the position estimates are accumulated. The results are for a normal distribution of errors in power measurements with a standard deviation of 20% (0.02). This shows the performance of the two ways of combining the position estimates obtained from different neighbors using aligned directional antennas. The two methods are performing aggregation of multiple sample values using averaging (one Align) and using error resilient triangulation (one Align LSE). We observe that one Align is at least two times more accurate than one Align LSE. One of the primary reasons for this phenomenon is that the formulation of error resilient triangulation discards angle information that is retained in averaging. It is important to note that in this set up ERT is not equivalent to an optimal least square estimate of location. This is because the ERT method gives the optimal solution when range estimates are the only constraints on the system. Because of our method of solving for location with directional antennas, we can estimate the relative angle between the anchor and the sensor node in addition to the inter-node distance. This gives range as well as angle constraints. So the solution derived using only range constraints is no longer optimal and hence the use of the term least square estimate for it can be regarded as a misnomer. As averaging performs better than ERT for directional antennas, we use averaging as the method of aggregating results obtained from neighbors for the other schemes.

Fig. 4.9 shows the error in location determination for the three directional antenna schemes along with the scheme for omni-directional antennas. The most important observation here is that the curve for omni-directional antennas is distinctly higher than all the directional antenna curves. This shows that error in location determination can almost be reduced to half of its original value by using one of the proposed schemes based on directional antennas. So, a location determination protocol based on the proposed schemes using directional antennas can give more accurate location estimates compared to a similar protocol based the ERT scheme using omni-directional antennas.

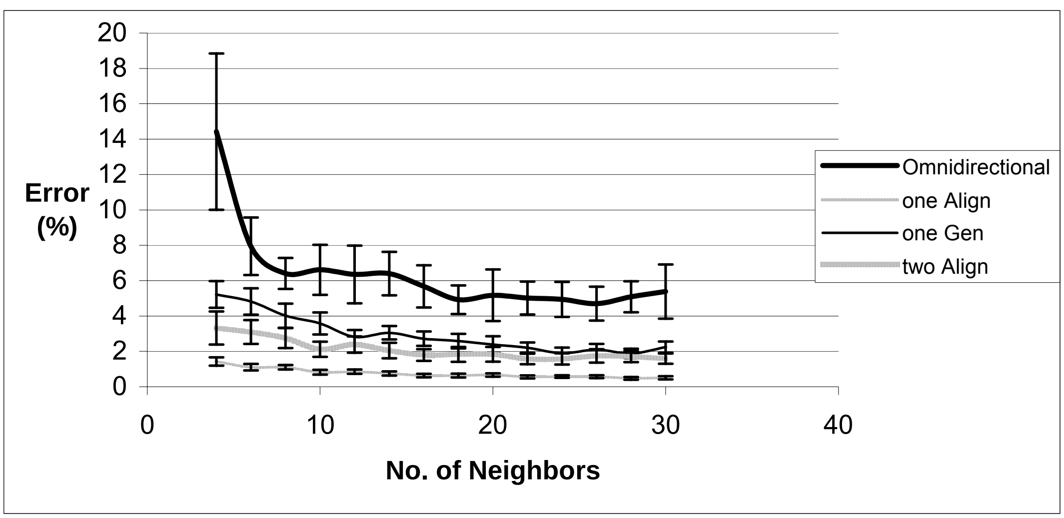

Fig. 4.9 Comparison of location determination error using different schemes.

The performance of the scheme using two anchors with aligned antennas is observed to be comparable to the scheme using one anchor with aligned antennas. This is a promising result as it shows that small sensor nodes can be localized almost as accurately as larger nodes, at the expense of employing a second anchor. The scheme for general antenna orientation also has a tolerable error that is lower than the omni-directional antenna based method. This shows that directional antennas can also be deployed in environments where it is not possible to align all the nodes without adversely affecting the performance of location determination protocols.

The curves for directional antennas are also flatter compared to that for omni-directional antenna. The omni-directional antenna based scheme has a knee point at 10 neighbors. This suggests that for reasonable accuracy in location determination the sensor density should be maintained such that each sensor node has at least 10 neighbors. The schemes based on directional antennas do not have such a sharp knee point and thus the location determination error at low sensor densities is not significantly worse compared to the error at higher sensor densities. This suggests possible cost savings from reduction of investment in hardware arising out of a lower sensor density.

Fig. 4.10 shows a plot of the error in ERT based location determination obtained by using three different range estimation techniques. The error for the directional antenna based techniques is still significantly lower than the error for the omni-directional antenna based technique. This shows that the performance improvement observed in Fig. 4.9 is not an artifact of the difference in the method using for aggregating location estimates obtained from neighboring anchors. All the curves in Fig. 4.10 have been obtained by discarding angle information and only range estimates have been used for ERT. The fact that directional antennas still perform better shows that the directional antenna based schemes proposed in this thesis give inherently better range estimates compared to omni-directional antenna based methods. This highlights a critical distinction between the set of techniques based on omni-directional antennas and the proposed schemes based on directional antennas. The received signal strength measurements with directional antennas have inherent angle information which is absent in measurements obtained from omni-directional antennas. Using this information in an intelligent fashion, as done in the proposed techniques, can significantly improve the accuracy of location determination.

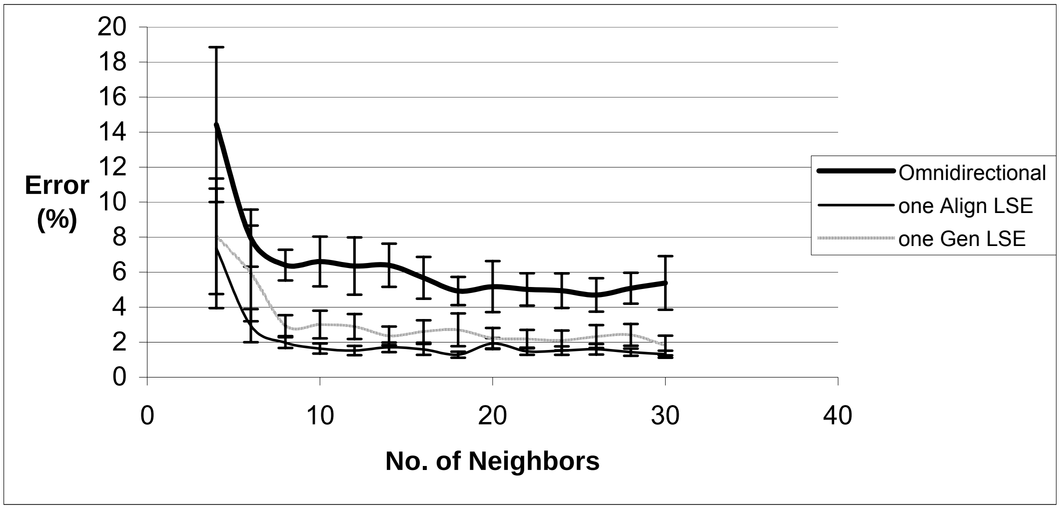

Fig. 4.10 Comparision of ERT based location estimates using directional and omnidirectional antennas

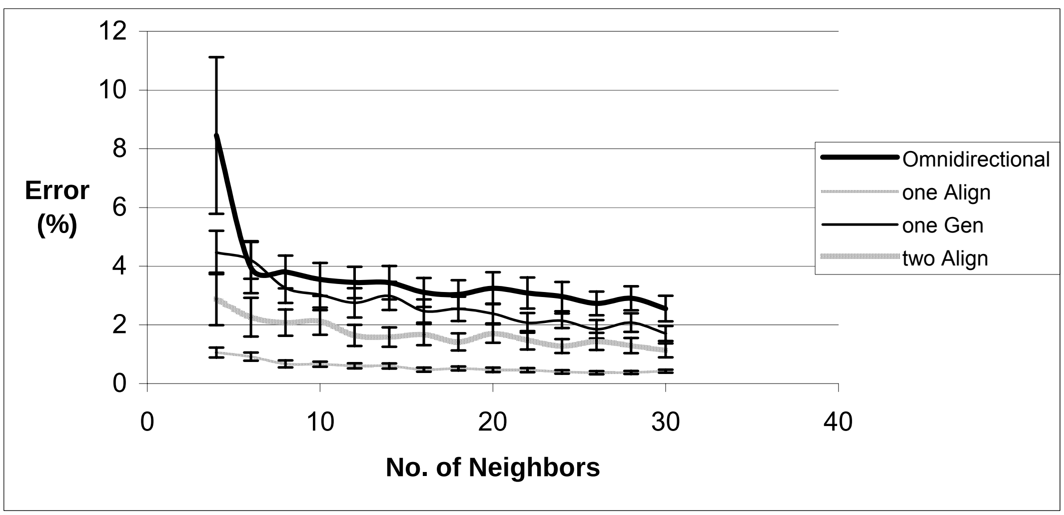

Fig. 4.11 Location determination error for uniform distribution of errors in power measurements.

All the results reported earlier were based on a normal distribution of errors with a variance of 20%. Fig. 4.11 shows the curves for a uniform error distribution ranging between $\pm 20\%$. As can be seen, the observations made earlier hold true for this model of error distribution as well.

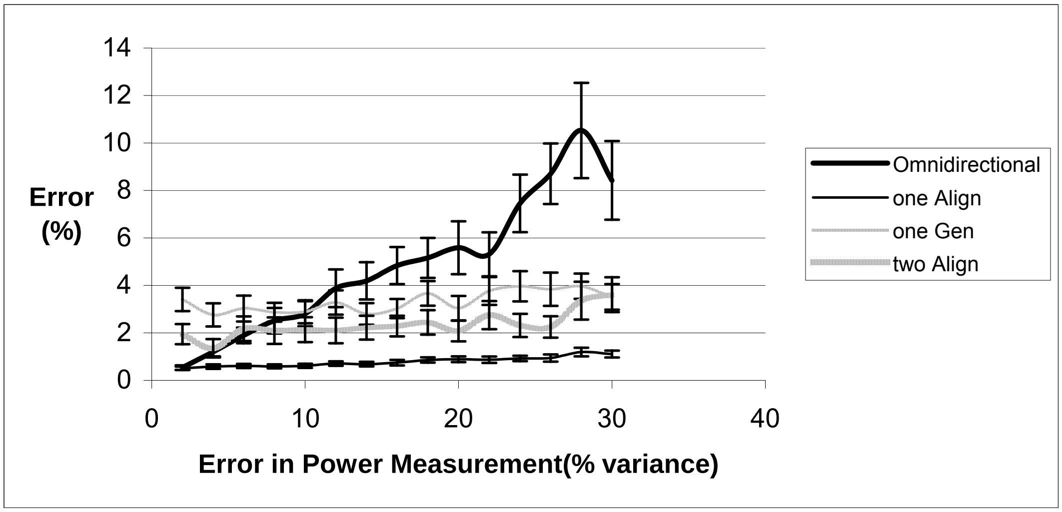

Fig. 4.12 Variation in location estimation error with error in power measurements

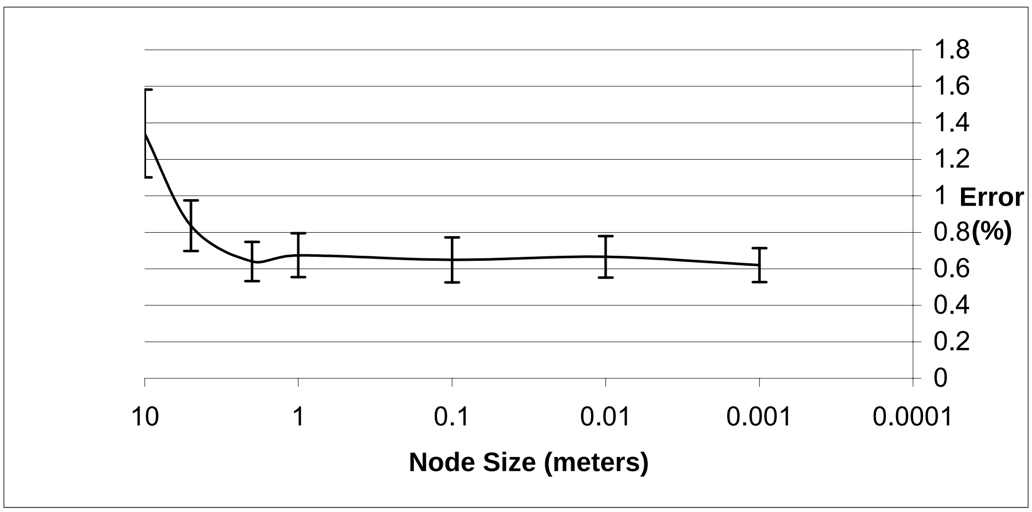

Fig. 4.13 Dependence of estimation error on node size

In the next set of experiments the effect of error in the received power measurements on the accuracy of location estimation was studied. For this experiment the number of neighboring anchor nodes was fixed at 10 anchors. Fig. 4.12 shows that the estimation error in all the schemes increases as the distortion in power measurements increases. It is also observed that directional antenna based schemes have a more graceful degradation in performance with increasing distortion in received power compared to the omni-directional method. Using our location determination methods for directional antennas, the error in position estimation is only 1-4% of the transmission range for 30% variability in the received power but for omni-directional antennas the error is 10%. For any received signal strength based location determination scheme it is necessary to use a model for the attenuation of signal strength with distance. The actual values of received signal strength in practice may differ from the values predicted by the antenna model. Fig. 4.12 shows that the proposed directional antenna based schemes are more robust to such errors in power measurements compared to the omni-directional antenna based ERT scheme.

Fig. 4.13 shows the contribution of node size to error rate. This experiment was done for the single, aligned anchor node case with 10 neighbors and normal distribution of errors in power measurements with a variance of 20%(0.02). As the size increases, the error rate of the location determination protocol increases. Also, as the node size becomes smaller than 1 meter, the error rate levels off. The bigger nodes have a higher error rate because of a *shielding effect*. It is more likely that a sensor node and an anchor node are lined up such that the signal from the transmitting antenna on the anchor cannot reach the two receiving antennas it needs to communicate with on the sensor node. A smaller node presents less shielding effect and therefore, the transmitting antenna can usually reach both antennas. It should also be noted that while our model flattens out as the node size approaches zero, it is unlikely that a real-world model would behave similarly as the size continues to decrease. As the node size approaches the wavelength of the transmitted signal, the received power at the antennas becomes difficult to model and their ability to give useful data in location determination would decrease greatly.

5. CONCLUSION AND FUTURE WORK

The work in this thesis attempts to illustrate the different aspects of the problem of location determination in ad-hoc and sensor networks. We started with an investigation of the influence that network characteristics have on the ability of middleware location determination protocols to accurately estimate position of sensor nodes. We presented a simulation based study that demonstrated the strong relationship between a network's topology and the performance of location determination protocols. Our work also demonstrated how intelligent control over the motion of network nodes can improve the accuracy of location estimation by up to 50%. The significance of this result lies in allowing a network designer to make a suitable tradeoff between QoS of location determination and other application protocols while choosing a network topology or motion pattern.

In the second part of this work, we shifted our focus to extending the available location determination methods for use with directional antennas. A set of three range estimation techniques using directional antennas was developed. Together these techniques cover most of the common deployment scenarios for sensor networks. We provide an account of the tradeoffs among these schemes, such as freedom of orientation versus beam width and node size versus number of anchor nodes. We do not propose a protocol for location determination with directional antennas. Instead, we provide a previously unavailable tool for range estimation using measurement of the received signal strength with directional antennas. This can form the foundation of new and more efficient location determination protocols.

The simulation carried out for evaluating the performance of the proposed schemes demonstrated some advantages that directional antennas have over omni-directional antennas. It was shown that the range estimates obtained using directional antennas are more accurate than those obtained using omni-directional antennas. The error in position estimates obtained using directional antennas was found to be half of the error in position estimates obtained using omni-directional antennas. Moreover, directional antenna based techniques exhibited less performance degradation under adverse conditions like low sensor density and error in power measurements. It should also be noted that a single location estimate using omni-directional antennas requires three neighbors and hence a transmission of at least three messages. The proposed schemes using directional antennas, on the other hand, require only one (aligned antenna case) or two message transmissions (general case and two anchor case). This suggests the possibility of significant energy savings in power constrained sensor networks. These observations show the potential that directional antennas have for providing a robust and accurate solution for location determination in sensor networks. The techniques proposed in this thesis are the preliminary steps in this direction that provide the groundwork necessary for future research in this promising area.

As part of future development of this work, we intend to extend the scheme using two anchors with aligned antennas for general deployment of nodes with possibly unaligned antennas. The proposed techniques in their current form use numerical methods for solving systems of non-linear equations. To avoid this computational expense we intend to explore possible ways of linearizing these equations to arrive at a closed form solution. Finally, we want to develop a location determination protocol to exploit the potential advantages of the proposed schemes like less message transmissions and more robustness to low sensor densities and high power measurement errors. We intend to implement such a protocol on a test-bed and experimentally verify the efficacy of the proposed schemes. This will also involve a study of the sensitivity of the schemes to the correlation in the error in power measurements at multiple receiving antennas on a sensor node.

LIST OF REFERENCES

LIST OF REFERENCES

[1] Philo Juang, Hidekazu Oki, Yong Wang, Margaret Martonosi, Li-Shiuan Peh, and Daniel Rubenstein, "Energy-efficient computing for wildlife tracking: design tradeoffs and early experiences with ZebraNet," in *International Conference on Architectural Support for Programming Languages and Operating Systems*, October 2002 pp. 96-107.

[2] J. M. Kahn, R. H. Katz and K. S. J. Pister, "Mobile Networking for Smart Dust," in *ACM/IEEE Intl. Conf. on Mobile Computing and Networking (MobiCom 99)*, Seattle, WA, August 17-19, 1999.

[3] "Technical Specifications for Garmin's eTrex," available at http://www.garmin.com/products/etrex/spec.html

[4] Andy Harter, Andy Hopper, Pete Steggles, Any Ward, and Paul Webster, "The anatomy of a context-aware application," in Proceedings of the *5th Annual ACM/IEEE International Conference on Mobile Computing and Networking (Mobicom 1999)*, Seattle, WA, August 1999, pp 59-68.

[5] N. B. Priyantha, A. Chakraborty, and H. Balakrishnan, "The cricket location-support system," in *Mobile Computing and Networking*, 2000, pp 32-43.

[6] Serdar Cabuk, Nipoon Malhotra, Longbi Lin, Saurabh Bagchi , Ness Shroff, "Analysis and Evaluation of Topological and Application Characteristics of Unreliable Mobile Wireless Ad-hoc Network," in *10th IEEE Pacific Rim Dependable Computing Conference (PRDC '04),* March 2004.

[7] Chris Savarese, Jan Rabaey, Koen Langendoen, "Robust Positioning Algorithms for Distributed Ad-Hoc Wireless Sensor Networks", *USENIX Technical Annual Conference*, Monterey, CA, June 2002.

[8] Y. Chen, H. Kobayashi, "Signal strength based indoor geolocation," in *IEEE International Conference on Communications*, May 2002.

[9] P. Bahl and V. Padmanabhan, "RADAR: An In-Building RF-Based User Location and Tracking System," in *IEEE INFOCOM*, Israel, Mar. 2000.

[10] S. Capkun, M. Hamdi, J. P. Hubaux, "GPS-free positioning in mobile as-hoc networks," in *Hawaii International Conference on System Sciences (HICSS-34)*, January 2001, pp 3481-3490.

[11] D. Niculescu and B. Nath, “Ad-hoc positioning system,” in *IEEE GlobeCom*, November 2001.

[12] C. Savarese, J. Rabaey, and J. Beutel, “Locationing in distributed ad-hoc wireless sensor networks,” in *IEEE International Conference on Acoustics, Speech and Signal Processing (ICASSP)*, May 2001, pp 2037-2040.

[13] D. Wood and J. A. Stankovic, “Denial of service in sensor networks,” in *IEEE Computer*, October 2002, pp 54–62.

[14] J. Preiss et al., “Polarization diverse antenna for portable communication devices,” U.S. Patent 6 031 503, 2000.

[15] Jan Beutel, Geolocation in a PicoRadio Environment, M.S. Thesis, ETH Zurich, December, 1999.

[16] M. A. Jensen, and Y. Rahmat-Samii, “Performance Analysis of Antennas for Handheld Transceivers Using FDTD”, in *IEEE Trans. Antennas and Propagation*, vol - 42, August 1994, pp. 1106-1113.

[17] Paolo Santi, Douglas M. Blough, Feodor Vainstein, “A probabilistic analysis for the range assignment problem in ad hoc networks”, Proceedings of the *2001 ACM International Symposium on Mobile ad hoc networking & computing (Mobihoc)* 2001.

[18] Christian Bettstetter, “On the minimum node degree and connectivity of a wireless multihop network”, Proceedings of the *third ACM international symposium on Mobile ad hoc networking & computing (Mobihoc)*, 2002.

[19] S. Shakkottai, R. Srikant, N. Shroff, “Unreliable Sensor Grids: Coverage, Connectivity and Diameter”, *INFOCOM 2003*, April 2003.

[20] A. Howard, M.J. Mataric, G.S. Sukhatme, “Mobile Sensor Networks Deployment Using Potential Fields: A Distributed, Scalable Solution to the Area Coverage Problem,” in *6th International Symposium on Distributed Autonomous Robotic Systems*, June 2002.

[21] Z. Butler, D. Rus, “Event-Based Motion Control for Mobile-Sensor Networks,” in *IEEE Pervasive Computing,* April 2003, vol 2, pp 34-42.

[22] G. Wang, G. Cao, T.F. La Porta, “A Bidding Protocol for Deploying Mobile Sensors,” in *IEEE International Conference on Network Protocols*, November, 2003.

[23] Jeffrey Hightower and Gaetano Borriello, “Location sensing techniques,” Technical Report of the University of Washington Computer Science Department, UW-CSE-01-07-01, July 2001.

[24] J. Hightower and G. Borriello, “Location systems for ubiquitous computing,” in *IEEE Computer*, August 2001, pp 57-66.

[25] Andy Harter, Andy Hopper, Pete Steggles, Any Ward, and Paul Webster, “The anatomy of a context-aware application,” in Proceedings of the *5th Annual ACM/IEEE International Conference on Mobile Computing and Networking (Mobicom 1999)*, August 1999, pp 59-68.

[26] N. Bulusu, J. Heidemann, and D. Estrin, “GPS-less low cost outdoor localization for very small devices,” in *IEEE Personal Communications Magazine*, October 2000, pp 28-34.

[27] J. Hightower, R. Tower, and G. Borriello, “SpotON: An indoor 3d location sensing technology based on RF signal strength,” Technical Report of the University of Washington, Computer Science Department, February 2000.

[28] N. Sundaram and P. Ramanathan, "Connectivity based location estimation scheme for wireless ad hoc networks," in Proceedings of *Globecom*, vol. 1, Nov. 2002, pp.143-147.

[29] L. Doherty, L. El Ghaoui, K. S. J. Pister, “Convex Position Estimation in Wireless Sensor Networks,” in *Infocom 2001*, April 2001.

[30] Kay Römer, “The Lighthouse Location System for Smart Dust,” in *MobiSys 2003* (ACM/USENIX Conference on Mobile Systems, Applications, and Services), May 2003.

[31] “The Network Simulator – ns-2” available at http://www.isi.edu/nsnam/ns

[32] P.J.B. Clarricoats, Y. Rahmatt-Samii, J.R. Wait, “Handbook of Microstrip Antenna,” in *IEEE Electromagnetic Waves Series 28*,volume 1, 1989.

[33] M. Vossiek, L. Wiebking, P. Gulden, J. Wieghardt, C. Hoffmann, P. Heide, “Wireless local positioning,” in *IEEE Microwave Magazine*, Volume: 4, Issue: 4, Dec. 2003, pp 77-86.